High Stress Uniaxial Tensile Fatigue of Plain Concrete as it Pertains to Offshore Wind Turbines

A thesis submitted by

Connor Brown

In partial fulfillment of the requirements for the degree of

Master of Science

In

Civil and Environmental Engineering

Tufts University

August 2017

Abstract

High Stress Uniaxial Tensile Fatigue of Plain Concrete as it Pertains to Offshore Wind Turbines

Nonrenewable energy is currently the main power source of energy for the United States. Using nonrenewable resources at current levels is detrimental to the environment and is not a long-term solution to providing energy for humankind. Renewable energy such as wind energy has great potential to replace or dramatically reduce the country's dependence on these nonrenewable energy sources. Offshore wind energy offers a good solution for coastal regions to reduce the dependence on these nonrenewable energy sources. Substantial research and development is needed to support efforts for design and construction of offshore wind turbines to have design lives that make their construction and use economically viable. The objective of this thesis is to further an understanding of the high stress tensile fatigue strength of plain concrete, primarily through uniaxial tensile tests. The results of these tests were analyzed and combined with previous data in this area to develop a better understanding for the response of plain concrete in high stress to low cycle loading.

Acknowledgements

First, I would like to thank God, as nothing would be possible without Him. I have leaned on His support throughout this entire process and I will continue to lean on Him as I move forward.

Second, I would like to thank my academic advisor Professor Dan Kuchma for his interest in this work and his technical support. I thoroughly enjoyed that our relationship encompassed more than engineering and that we were able to discuss politics and sports. It humanized the whole process and reduced the stress that a journey like this can create. I would like to thank my thesis committee members, Professors Brian Brenner and Babak Moaveni for their comments, critiques and flexibility. I look forward to maintaining relationships with them beyond the past five years I've spent at Tufts.

I would like to thank Laura Sacco for continually bailing me out when I missed deadlines and completing forms I had to sign. She was my mother away from home and I looked forward to our daily conversations about non-engineering topics. I will cherish those memories.

Next, I would like to thank my fellow officemates, Jordan Weinstein, Nate Davis, Sofia Puerto and Wenjian Lin for their knowledge, support and most importantly good senses of humor. Tight office space is better shared with good friends and supportive colleagues. I look forward to seeing each of you have great success in life, wherever your paths may lead.

To all of my friends over the past year who have worked with me, picked me up when times were difficult and enjoyed the high points, thank you. There would be too many names to list to accurately do justice to the tremendous support I have received from each of you. I am a lucky man to have you as my support group and I look forward to having more time to enjoy with you when I am not living in Anderson Hall.

To the Tufts Soccer coaching staff and team, thank you for winning a national championship and allowing me to wean off from being a student-athlete to a 5th string, washed-up assistant coach. It was an incredible ride and I was very blessed to have been on it with you over the past year. I can't wait to watch the games next year from grainy, pixilated video feeds and cheer you on from the sidelines.

Finally, I want to give a massive thank you to my family. Mom, Dad, and Genevieve have been so supportive and loving throughout all of my life. Words cannot do justice to how much you have helped me and shaped me into the person I am today.

Table of Contents

List of Tables

List of Figures

Chapter 1. Introduction

1.1 General Introduction to Offshore Wind

Nonrenewable energy is currently the main power source of energy for the United States. Using nonrenewable resources at current levels is detrimental to the environment and is not a long-term solution to providing energy for humankind. Renewable energy such as wind energy has great potential to replace or dramatically reduce the country's dependence on these nonrenewable energy sources.

Wind energy has been growing at a rate of 20-30% per year over the past decade and is the fastest growing energy resource globally [Musial]. This is because of increased attention to global warming, finite fossil fuel resources, and a decrease in the cost of wind energy, due to advances in technology. The majority of this growth has been onshore wind production, which is excellent for areas with open space to build wind farms, but not as well suited for coastal cities where space is limited. In order to power these locations offshore wind energy presents a solution for the United States as the United States has the second highest offshore wind potential in the world [Musal, Butterfield]. The technical potential for offshore wind at 5 to 50 nautical miles off the United States' coast is estimated to be more than 2,000 gigawatts (GW), which is enough to provide double the total demand for electricity of the United States in 2015 [Gilman]. Figure 1 displays the breakdown of the gross and technical resource capacity potential in different areas of the United States.

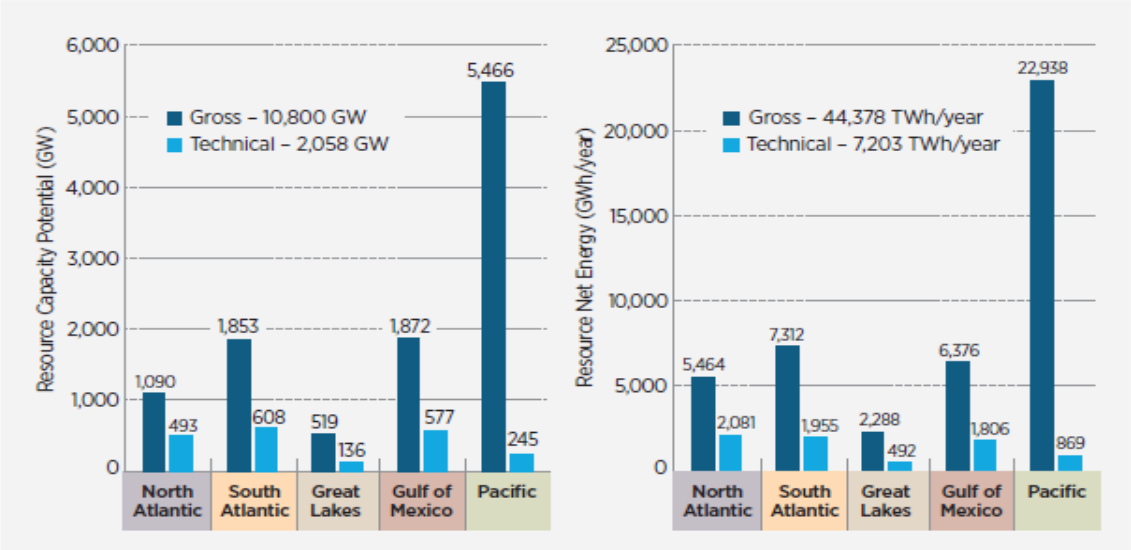

Figure 1 - Capacity (left) and net energy (right) of offshore wind resource estimates for five U.S. offshore wind resource regions [Gilman]

The most accessible wind resources are in the North Atlantic and South Atlantic locations. This is because of the signifcuant continental shelf that extends off the east coast of the United States.

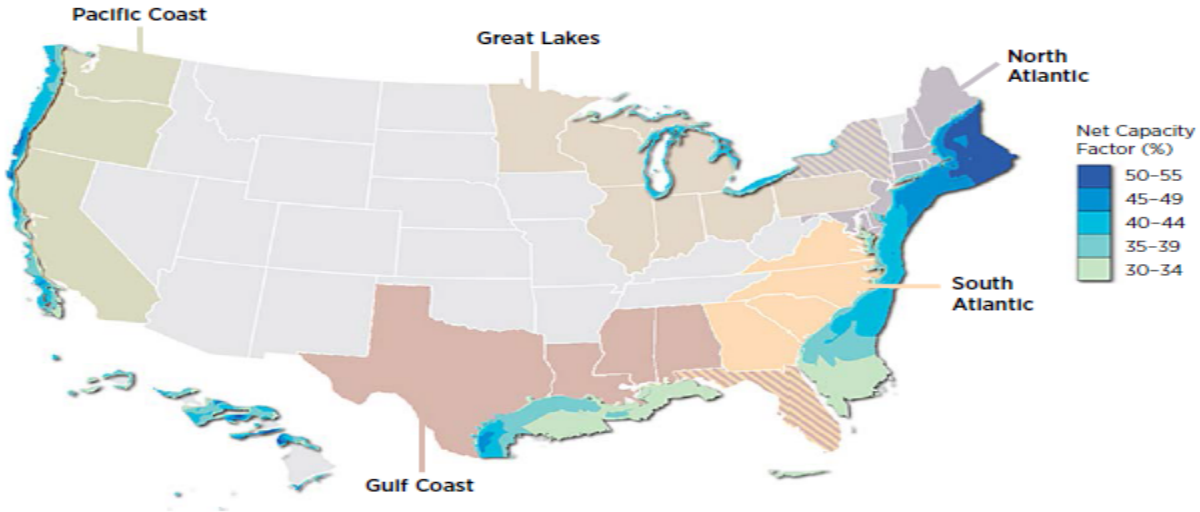

Figure 2 - Net capacity factor of offshore wind in United States [Gilman]

1.1.2 Offshore Wind Advantages and Disadvantages

Offshore wind has many advantages over onshore wind, which include the following [Musal, Butterfield and Henderson]:

- Wind blows more strongly and consistently, with less turbulence and smaller wind shear forces.
- The sea is undeveloped so there is ample space to place the turbines.
- This wind resource is in closer proximity to major coastal city centers, with greatly simplified transmission permitting requirements.
- Offshore turbines may be constructed to be much larger than onshore turbines and therefore there are fewer turbines needed for the same wind energy resource harnessing. This has significant economic advantages.
- Visual and noise disturbances can be avoided when turbines are placed sufficiently offshore.

Despite these benefits, offshore wind also has disadvantages relative to onshore wind, which include the following:

- The wind loads applied to the offshore wind turbines are far greater than those applied to onshore wind turbines. This increases the fatigue damage on the structure due to cyclic loading.
- A higher capital investment is required for offshore wind turbines because of the costs associated with marinization of the turbine and the added complications of the foundation, support structure, installation, and decommissioning.

- Offshore installations are less accessible than onshore installations, which raises the operations and maintenance costs and potentially increases the downtime of the machines.
- The presence of the dynamic loading from waves and from hurricanes further increases the complexity of the design and reduction in the fatigue life.

1.1.3 State Developments

Recently, individual states have been taking real actions to diversify their energy portfolios. In Massachusetts, legislation has been passed to help strengthen green energy standards. Governor Charlie Baker signed Bill H.4568 on August 8th, 2016. The bill is the most progressive energy bill for offshore wind to be passed in the United States and it requires the state of Massachusetts to have 1,600 Megawatts (MW) of energy producers in the next 10 years [Bill H.4568]. Constructed off the coast of Block Island in Rhode Island, the first U.S. offshore plant became operational in 2016. It is a modest farm with five, large 6 MW turbines. This wind farm can power approximately 17,000 homes [Schlossberg]. New York and California have also set lofty renewable energy goals. By 2030, these states plan to have 50% of their electricity generated from green energy [Gilman]. These two states have major population centers located along their coasts, which would make offshore wind turbines an attractive energy source. Hawaii was the first state to commit to a 100% Renewable Portfolio Standard in 2015, which means a total dependence on green energy [Gilman]. They pledge to be totally independent of fossil fuels by 2045.

1.1.4 Current Challenges with Offshore Wind Resource Development

Because offshore wind turbines are new to the United States, there are bountiful opportunities for research. Currently, the design of wind turbines is based upon the combination of previous knowledge of onshore wind turbines and offshore oil rigs. These don't serve as perfect matches though. Onshore wind turbines are not subject to loads as large as offshore wind turbines experience and they don't have to account for the corrosive properties of saltwater. Oil rig design does not have to account for the same magnitude of dynamic wind loading and the design life requirements are not the same. Oil rigs are designed to have lifespans of about 20 years. This is pertinent to the oil industry because the oil reservoirs are generally empty after a finite amount of years of mining them. Wind energy doesn't change significantly over long time horizons so increasing the design life of offshore wind turbines would allow them to harness more energy and generate higher profits for owners. Significant research is needed to create more efficient, longer lasting wind turbines. Understanding the fatigue properties of the material components used in wind turbines would help engineers to make more educated decisions when designing these structures. This thesis focuses on the properties of concrete in the turbines foundation when exposed to repeated tensile loadings.

1.1.5 Opportunities for Research Development

The United States is almost certainly going to develop significant offshore wind energy resources in the years to come at the state level, but there are many technical issues associated with offshore wind that need to be addressed. These issues include a lack of infrastructure, design regulations, installation experience, supply chain and workforce.

Currently, there is a large push in the United States for its public and private universities to advance research in theoretical and experimental data collection. This opportunity for research is where the subject of this thesis arose. This thesis attempts to delve into some of the gray area associated with uniaxial tensile fatigue in the concrete at the base of the turbine by understanding the material response of concrete to uniaxial tensile fatigue.

1.2 Offshore Wind Standards

Offshore wind energy is a relatively new enterprise in the United States and therefore offshore wind standards are immature. Currently, the Bureau of Ocean Energy Management is the primary regulator for offshore wind development in the United States, and the International Electrotechnical Commission (IEC) and the International Standards Organization (ISO) have jurisdiction over international design standards which may be used as well. The American Petroleum Institute (API) have industry specific design standards for oil and gas development. The most relevant design codes to this thesis are:

- IEC 61400-1, Wind turbines—Part 1: Design requirements
- IEC 61400-3, Wind turbines—Part 3: Design requirements for offshore wind turbines
- IEC 61400-3-2, Wind turbines—Part 3-2: Design requirements for floating offshore wind turbines (Pending)
- IEC 61400-22, Wind turbines—Part 22: Conformity testing and certification
- ISO 19900, General requirements for offshore structures
- ISO 19903, Fixed concrete offshore structures

- API RP 2A-WSD, Recommended practice for planning, designing and constructing fixed offshore steel platforms—working stress design.

Figure 3 shows where these design codes are applicable on the turbine.

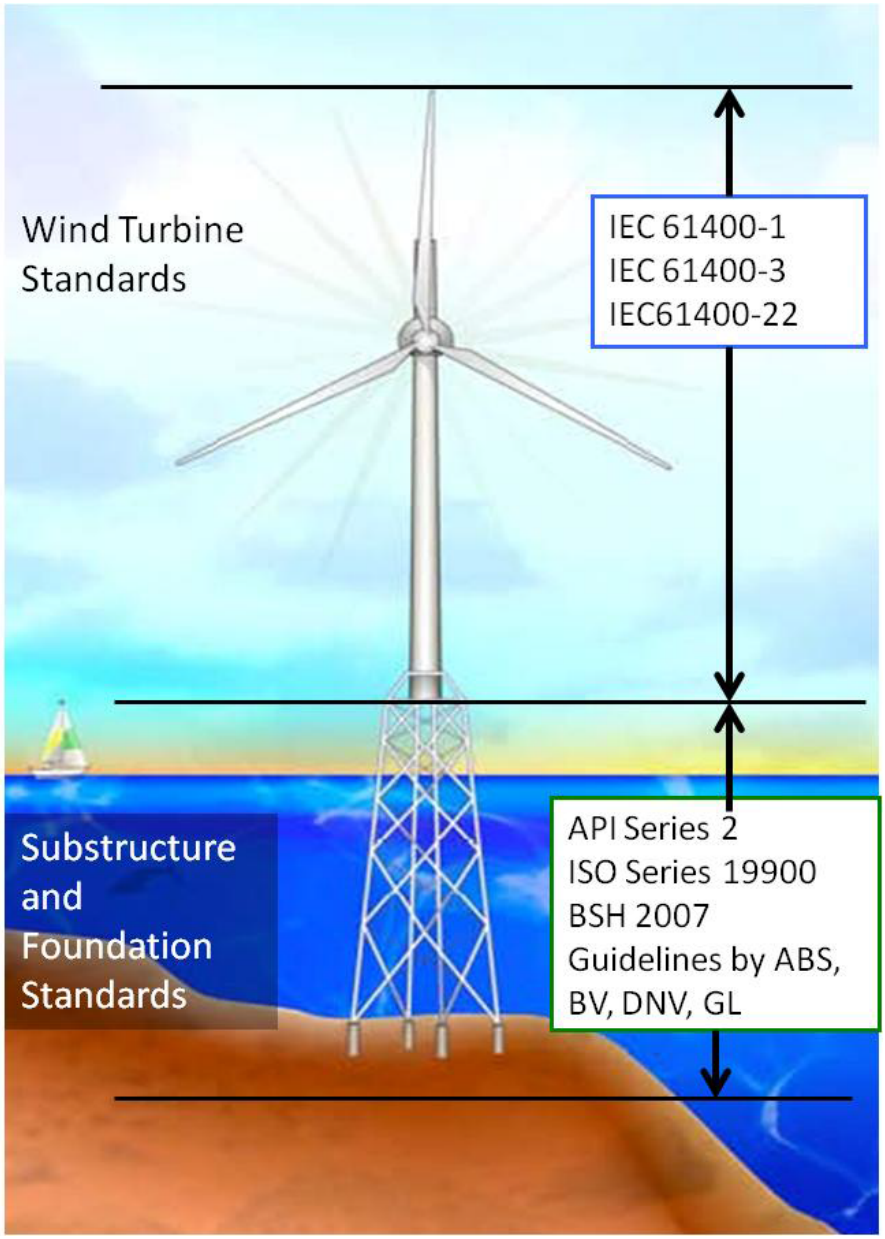

Figure 3 - Applicability of existing design standards for offshore wind turbines [Musial]

1.3 Cyclic Loading on Turbine

1.3.1 High Stress Low Cycle Loading

Extreme wind and wave loads are important loading conditions for design of offshore wind turbines. These conditions generally only occur in the presence of hurricanes or winter coastal storms, so understanding their patterns and likelihood of occurring are critical. For example, sample data from a US Army Corps of Engineers buoy station off the coast of Massachusetts reveals that the maximum wave height H_{mo} occurred in 10/31/1991, which is the date of "The Perfect Storm". The third highest wave height in the past 35 years occurred on 10/29/2012, which was Hurricane Sandy.

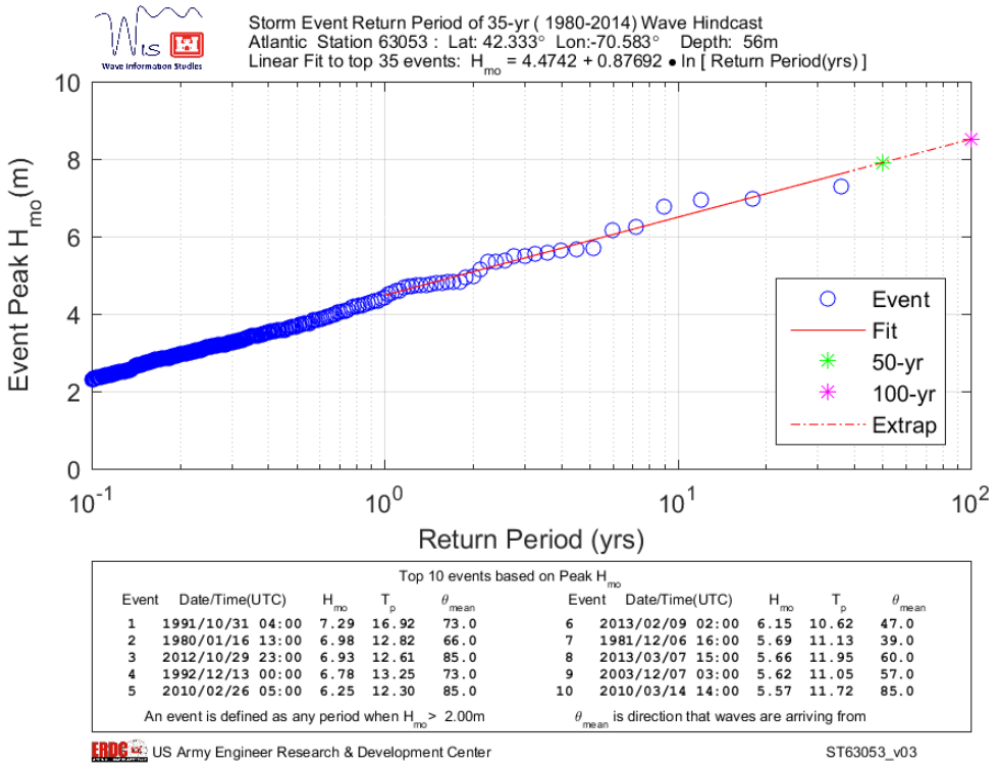

Figure 4 - Station 63053 maximum wave height in last 35 years [Wave Information Studies]

Fortunately for the offshore wind turbine community, the United States has been recording wind/wave information for decades and it is readily available to public and private companies. The three main databases are the Wave Information Studies Project by the US Army Corps of Engineers, a joint collaboration of the U.S. National Center for Environmental Prediction and the National Center for Atmospheric research, and Oceanweather. These databases have 20, 50 and 29 years of recording, respectively [ABS]. During a hurricane, an offshore turbine undergoes higher stresses than it would during regular operations, but only for a short duration. There is a small amount of research on high mean stress and low cycle concrete fatigue strength and this leads to gaps in knowledge in the research community. The work conducted through this thesis fills in some of that gap.

1.3.2 Low Stress High Cycle Loading

The other type of loading that turbines are subjected to during their lifespan is caused by low stresses at a high amount of cycles. This type of loading would include the passage of the blade when it is in motion and waves hitting against the base of the turbine. The turbine experiences hundreds of millions of these cycles throughout its 20-year operational life. This thesis does not investigate these loads.

1.4 Relevancy

The majority of offshore concrete turbines have shallow gravity foundations, which rely on a large block of concrete resting on the seabed floor to weigh the structure down and allow to remain upright [Offshore Wind Turbine Foundations].

Figure 5 - Offshore wind turbine gravity foundations

Concrete structures can crack easily in tension due to low tensile strength. This can expose the steel reinforcement to saltwater, which could lead to corrosion. The steel reinforcement carries the tensile force through the concrete and damaging this can lead a reduction in strength of offshore wind turbines. Corrosion also causes volume expansion, which exerts a radial pressure at the steel-concrete interface. This pressure can eventually lead to additional cracking and more exposure to corrosion. Understanding how concrete reacts to these higher tensile loadings that occur in offshore wind turbines is imperative to the advancement of the industry. This thesis does not investigate the entire structure, but instead focuses on the properties of the concrete from a fundamental material response level.

1.5 Objectives

The main objectives of this thesis are:

- Adding data to an understudied, but important topic of uniaxial tensile fatigue of concrete with a focus on the loading case of high mean stress.
- To design and evaluate the use of a simply uniaxial test setup for conducting fatigue tests
- To evaluate differences between the findings in this thesis and those from previous work.

1.6 Organization of Thesis

This thesis is organized in six chapters. Chapter 1 includes a general introduction to offshore wind energy, the challenges with the development of offshore wind energy, the loads applied to offshore wind turbines throughout their design life, and opportunities for research in this field in regards to tensile fatigue of concrete. Chapter 2 includes the literature review of uniaxial tensile fatigue of concrete. Chapter 3 details construction of the concrete specimen tested and the testing setup. Chapter 4 presents the data recorded from the 20 uniaxial tensile fatigue tests and includes observations on the data. Chapter 5 includes the conclusions from this thesis and suggests opportunities for research going forward.

Chapter 2. Literature Review

2.1 Introduction to Fatigue

Concrete is a widely used material and is often used in design situations that require it to withstand many cycles of loading during its lifespan. The behavior of plain concrete under repeated compressive loading has been extensively researched, but not in repeated tensile loading. Tensile fatigue tests of plain concrete have been investigated by means of bending [Raithby] and splitting tests [Tepfers]. These tests are easier to construct and carry out than uniaxial tension tests, but it is difficult to determine the actual stresses the specimens experience during the experiment because the stress is not distributed equally. Concrete in direct axial tensile fatigue is a method of testing that allows researchers to evaluate the stress throughout the sample, but it is seldom researched because it is difficult to create samples without having stress concentrations or bending of the specimens. A brief view of the literature reveals that several researchers have attempted to add data regarding uniaxial tensile fatigue, but there has not been significant research done investigating the response of concrete to high stress load cycle uniaxial tensile fatigue and therefore, this thesis endeavors to shed light into that discussion.

Fatigue is the weakening of a material due to repeated cyclic loads. Progressive damage occurs as the material is subject to high frequency, low loading (waves and winds) or low frequency, high loading (earthquakes and explosions). High-frequency, low-loading fatigue in concrete can cause failure at stresses that are much lower than the ultimate tensile strength. This progressive loading causes infinitesimal changes in stiffness each

load cycle and can lead to sudden failures without noticeable plastic deformation. Cyclic loading at high stress levels causes massive damage in concrete and an overview of this is included in committee reports of RILEM and ACI [Hawkins and Shah 1982; RILEM 1984; ACI 1982].

Microcracking isdetailed in the RILEM and ACI reports as well and is an important contributor to a loss of strength in concrete. Microcracking is tiny cracks that occur throughout the concrete specimens that are caused by cyclic loads. Microcracking has been shown to increase crack propagation at stresses that are 70% of the ultimate stress of the concrete [Shah and Chandra 1970].

2.2 Plain Concrete

Before discussing concrete's response to fatigue, it is important to explain the nuances of the material itself. Concrete is a non-homogenous material that is mainly composed of cement, aggregates and water. The ratios of each of these three materials, their properties, curing length, and method of mixing all play an important role in the performance of each batch of concrete under cyclic fatigue loading. Most concrete is reinforced because of its very limited tensile capacity. Plain concrete is concrete that has no steel reinforcement in it and is the subject of this research. According to RILEM, "the fatigue properties of concrete exposed to pure tensile stresses have not been studied extensively" which suggests significant opportunities for researching this area [RILEM]. The RILEM report continues saying "one reason for the lack of tensile fatigue tests is the practical difficulty in loading a specimen in tension without introducing stress concentrations of local

bending." Due to the non-uniformity in concrete and the fact that tensile failures in concrete are brittle and sudden, the test results for tensile strength vary significantly. Tensile strength is generally found to be 10 to 15% of compressive strength.

2.3 Fatigue in Uniaxial Tension

Uniaxial tension tests have the advantage that at every section cut of the concrete, independent of the heterogeneous nature of the material, the applied stress is largely the same. These tests are generally carried out in two loading patterns. The first is a load-controlled test, which is the procedure employed in this research study. In a load-controlled test, the amount of load applied to the specimen is preprogrammed and carried out despite deformations to the concrete during testing. This technique is effective for creating S-N curves and results in sudden brittle failures. The second is a displacement-controlled test, which allows the researcher to set a standard rate of displacement and requires a machine that is able to react quickly to accommodate for plain concrete's property to suddenly fail. This type of testing allows the researcher to see how much load the concrete can hold after the first cracks develop. This technique was not used in this thesis.

Although uniaxial tension seems to be the most logical choice when performing a fatigue test, issues associated with achieving uniform application of tensile stress on the concrete specimen have deterred many researchers from investing time in it. Some of these issues include, bending and torsion introduced because of incorrect construction of the concrete specimen. The author took extreme care in creating testing specimens to achieve a

reasonably uniform tensile stress distribution across the member sections. This is further addressed in the Chapter 3. In some tests, epoxy resins have been used by researchers to ensure a more even spread of stress on the specimens [Cornelissen 1982].

The literature describes a few tests where uniaxial tensile fatigue in concrete has been evaluated ([Cornelissen 1982, 1984, 1985], [Morris, A.D.], and [Kolias, S]). All of these tests were conducted under constant amplitude loading except for a small partition of the tests explored by [Cornelissen 1985]. These tests focused on concrete with different mixes, curing conditions and for different values of maximum and minimum stresses. The maximum tensile stress as impacted by fatigue ranged from 70% to 87.5% of the static tensile strength and the minimum stress ranged from 0% to 40% of the static tensile strength and 5% to 30% of the elastic compressive strength.

2.4 Examination of Minimum Stress Applied

The study that is most pertinent to this thesis is research on fatigue behavior of plain concrete under uniaxial tensile loading at Delft University in the Netherlands by Cornelissen [Cornelissen 1982, 1984, 1985]. Similar to the goal of this thesis, the objective of this research was to determine the number of cycles to failure of concrete when subjected to various stress levels. The results of this research can be summarized in Figure 6 below.

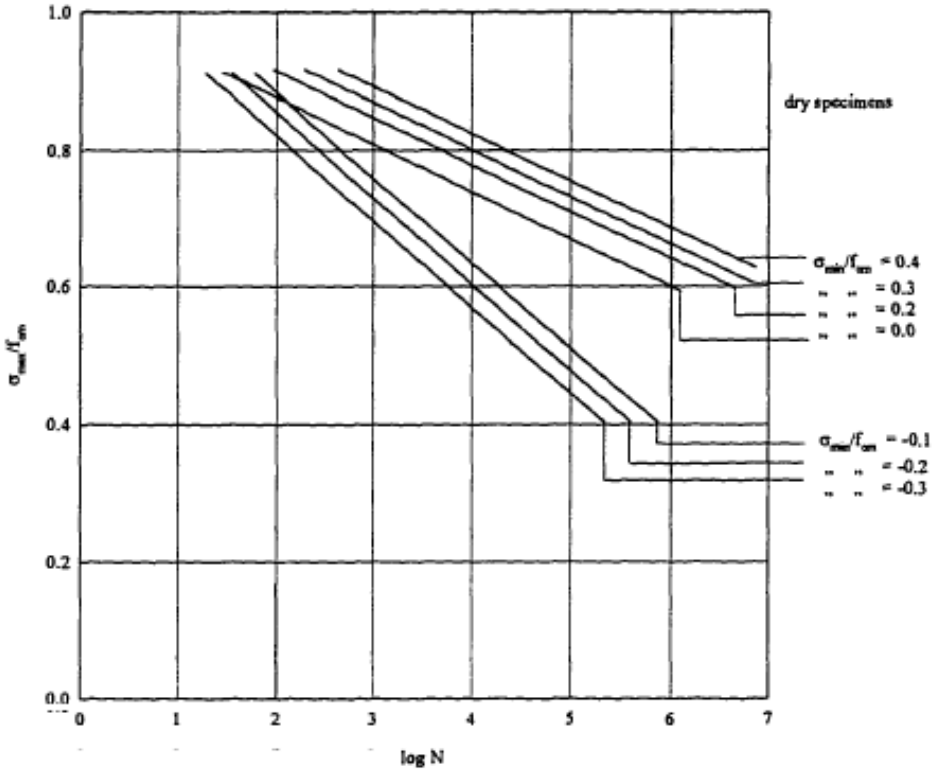

Figure 6 - Average S-N curves, for various lower limits, for concrete subjected to pulsating tension or to alternating tension-compression [Cornelissen 1982]

The x-axis is the log of the number of cycles until failure, the y-axis is the maximum stress applied divided by the maximum stress capacity of the concrete and the various trend lines represent the different minimum stresses applied over the stress capacity of the concrete. There is clearly a trend between increased loading and a decreased number of cycles required for failure. Another clear trend is when the stress range of testing was increased (minimum stress was decreased) the number cycles to failure decreased as well. There is a great reduction in life once the stress loading applied to the concrete varies between tension and compression, as the grouping of the three lines with negative stress applied over stress capacity represents. This thesis will not examine the effects that

compressive loading has on a specimen, but will seek to add to the data and analysis that Cornelissen produced.

2.5 Uniaxial Fatigue Response

There are two basic approaches in determining the uniaxial fatigue strength of concrete, empirical S-N cycle method and fracture mechanics. The S-N Cycle method [Miner] relies on simple assumptions and is used by designers because it is easy to understand, test and put into practice. The fracture mechanic method is more realistic and relies on crack propagation study.

2.5.1 S-N Curve (Wohler curve)

The S-N curve is an approach that has been used for decades to evaluate the fatigue capacity of many engineering materials. The main premise of this approach is that a single load is cyclically applied to a sample. Upon failure of the specimen, the number of cycles it took to fail, N, is recorded. If a greater magnitude of load is applied, the sample should fail at a smaller number of cycles N. Conversely, if a smaller magnitude of load is applied, it is expected that the sample can resist more cycles of loading before failure. Fatigue strength is defined as the fraction of the static strength that can be supported repeatedly for a given number given number of cycles. Concrete generally has a very large scatter in fatigue strength testing in part because of the lack of uniform static strength. Real structures do not follow these assumptions because they are not subject to a constant loading over their lifespan. Therefore, fatigue design typically involves conservative assumptions about reductions of material strength, with applications of

factors of safety applied both to loads (assumed increased) and resistance (assumed decreased).

2.5.2 Fracture Mechanics

The second approach uses fracture mechanics to study crack propagation owing to fatigue loading. Fracture mechanics takes the crack length increment increase per load cycle to applied stress intensity factor amplitude. This is more commonly used in the fatigue of metals and was first proposed by Paris [1963] who discovered that crack propagation da/dN could be related to the cyclic stress intensity factor (ΔK). $da/dN = \alpha (\Delta K)^{\beta}$, $(DeltaKI)=K_{max}-K_{min}$. α and β are empirical constants. See Figure 7.

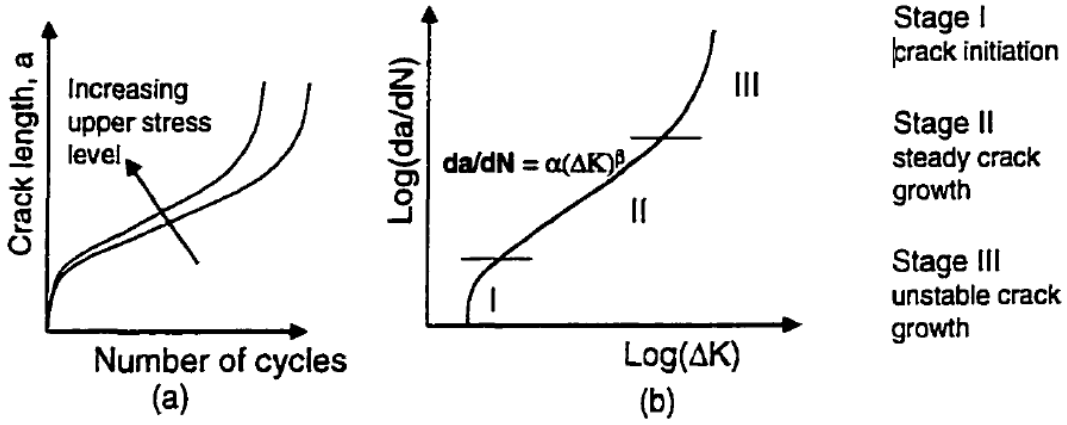

Figure 7 - Fracture mechanics approach for modeling fatigue response; (a) crack length vs. number of cycles for different upper stress levels, (b) rate of crack growth vs. range of stress intensity factor [Paris 1963]

Total fatigue life is based on the crack propagation state and the crack initiation stage. Fatigue analysis of the first stage is traditionally used with the S-N curve approach, AASHTO 2012; Goode and van de Lindt 2007), while the crack propagation phase is

analyzed using different models. The most common model is the "Paris Law" (Paris and Edorgan 1963).

2.6 Fatigue Limit

Fatigue limit is the stress level below which there will be no fatigue failure for any number of cycles and stress ratio. Steel and many metals have fatigue limits, but according to the ACI Committee 215 (1974) concrete does not have a fatigue limit. This is because metals are generally a continuous material and when loaded below a certain fatigue limit, they will not deform. Concrete is not a continuous material and is made up of a mix of different materials. When concrete undergoes loading, there is always going to be some deformation. The fatigue limit of concrete is generally found from cyclic loading and plotting the results on an S-N curve.

2.7 Gaps in Knowledge

Throughout the history of research on fatigue in plain concrete there was been a debate between how relatable flexural bending and axial fatigue tests can be. Because of the difficulty of axial tensile fatigue tests, a relationship would be beneficial to the scientific community. According to a study done at the University of Illinois at Urbana-Champaign by John W. Murdock on a review of research in the field of fatigue on plain concrete, he said he is "not convinced of the validity of this assumption," in relating flexural and axial tensile fatigue tests. He goes on to say that it "tacitly implies that a stress or strain gradient has no effect on the fatigue response of concrete. Such an implication has yet to be investigated, let alone proved" [Murdock, 2007]. Based on this relatively recent

publication, and the limited work in axial tensile fatigue tests at high stress/low cycle testing, there remains a need to verify and further explore high stress/low cycle fatigue, especially with its current relevance to offshore wind turbines experiencing these loads throughout their design lifespans.

Chapter 3. Preparation for Testing

3.1 Introduction

Precise specimen preparation and documentation for experimental testing is always of paramount importance to produce reliable results. With all of the previously documented challenges with testing in uniaxial tensile fatigue, most specifically the need to create specimens that are do not experience bending or torisional stress when loaded, the author took extra precautions to ensure the specimens were a uniform size. The following sections address the processes that were followed and demonstrate the accuracy in which the specimens were tested.

3.2 Specimen Layout

3.2.1 Concrete Specimen

The specimen that was used for this thesis was a 2-7/8th" x 4"x 18" concrete block that had 8, 5/16" threaded rods cast into it. These rods measured 7" and 5" in length and were offset so that the stresses on the specimen were symmetrical. These threaded rods connected to a steel plate with nuts and washers, which in turn connected to the Instron 8501 machine from a 3/4" threaded rod. The specimen and rod layout can be seen in Figure 8 and Figure 9.

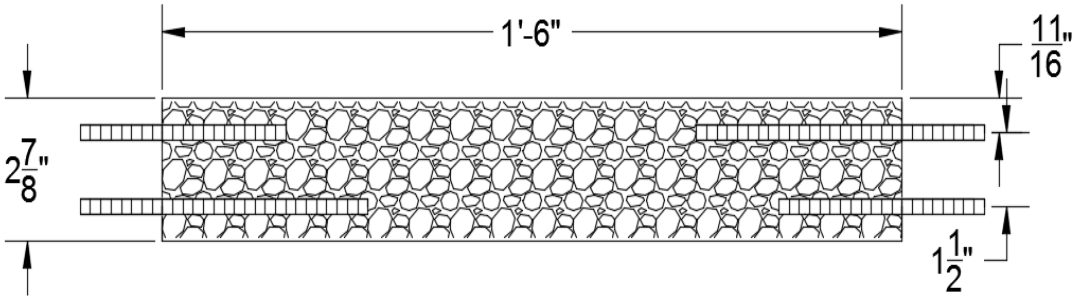

Figure 8-Elevation view of specimen

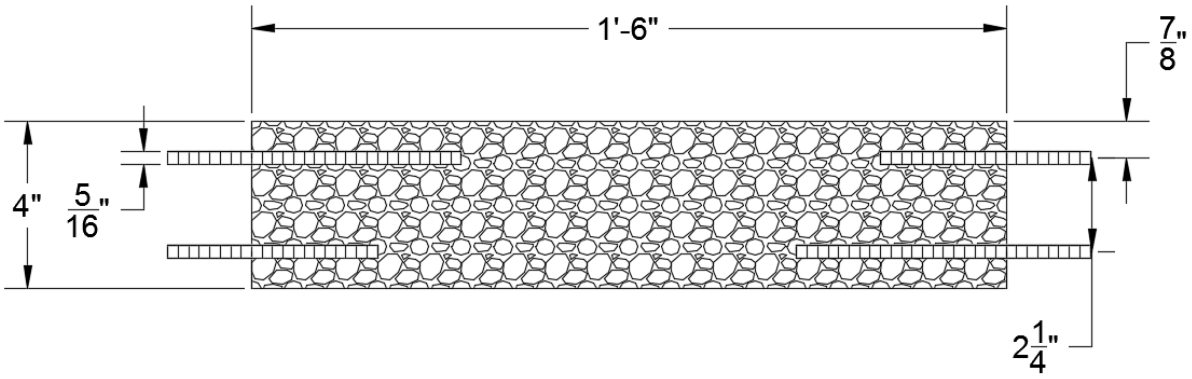

Figure 9 – Plan view of specimen

The specimen connection to the Instron testing machine can be seen below.

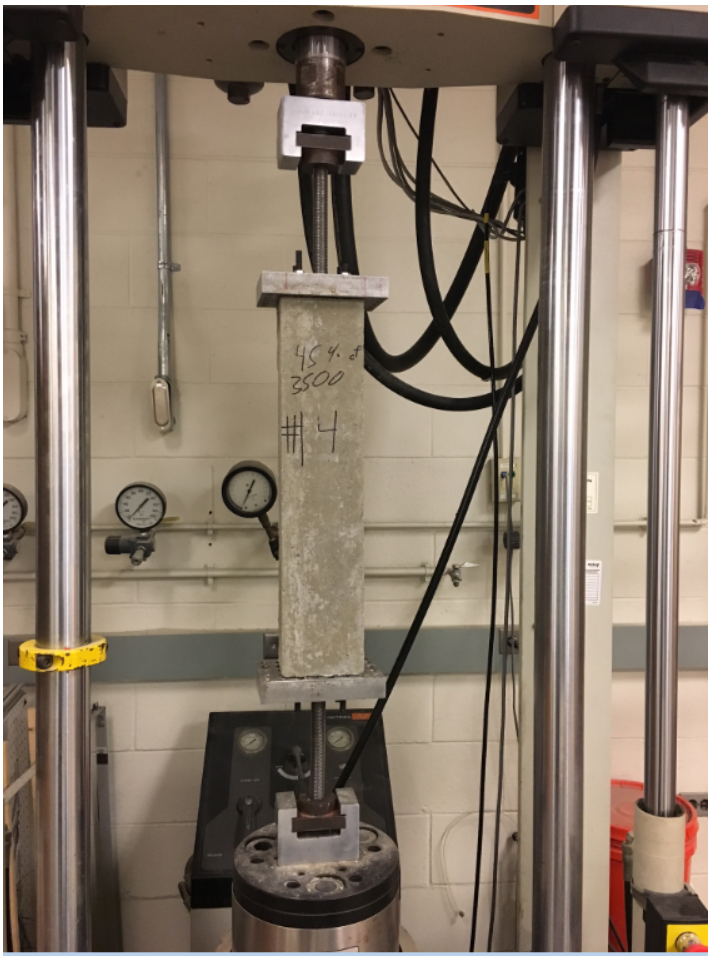

Figure 10 - Specimen in Instron 8501

3.2.2 Metal Plates

The metal plates were used to attach the rebar to the Instron machine. The end plates were 4” by 6” and the layout of the holes can be seen in Figure 11. The red holes were through which the rebar was inserted in order to attach the concrete specimen to the metal plate.

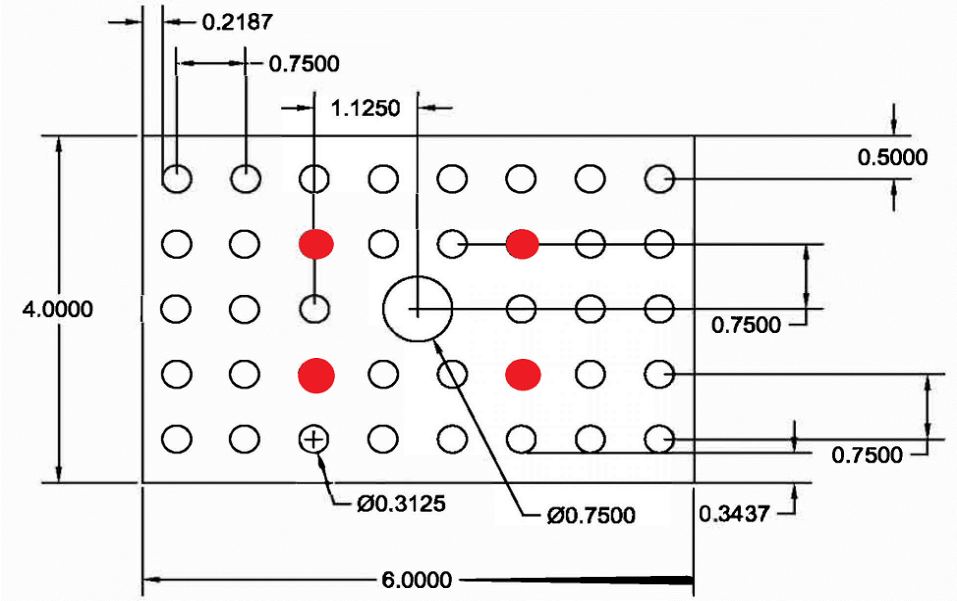

Figure 11 – Specimen metal plate

3.3 Specimen Construction

When constructing concrete specimens, the mold into which the concrete was poured dictated the shape of the specimen. For this reason, care was taken when assembling the molds. As can be seen in Figure 12 this thesis used three identical molds that were 2-7/8th" by 4" by 18" long.

Figure 12 - Freshly poured concrete in specimen molds

They molds were cleaned after each new specimen was cast and if inconsistencies were discovered, new wood was cut to account for any warping or bending in the mold due to exposure to moisture. Before the concrete was poured, each dimension was checked to ensure that the specimen was the correct size. The end plates that were used to cast the rods in the concrete were originally made out of wood because they were easy to construct and inexpensive, but with time they began to warp and affect the results of these tests. Steel plates were then used to make each specimen as close to identical as possible. The errors that may have been induced by the warping of the wood end pieces will be discussed in the results section.

3.4 Mix Details

The concrete used in the study was a 4000 psi Ready-To-Use QUIKRETE Concrete Mix from Home Depot. Before beginning the experiment, four different bags of concrete mix

were compared in a concrete cylinder compression test to ensure that the strength values from each mix were close to each other. The values of these four tests can be seen below.

Table 1 - QUIKRETE mix 7 day compressive strength

Cylinder Number	**Maximum Compressive Value at 7 Day Strength (psi)**
Mix One	3,883
Mix Two	3,325
Mix Three	3,477
Mix Four	3,805

These values are all similar in strength to each other and the mix was deemed to be uniform throughout and therefore acceptable for testing.

The QUIKRETE mix was sieved to remove the larger aggregate sizes, which could interfere with the tensile fatigue strength of the specimen. The No. 4 sieve was deemed to be the appropriate size for maximum strength according to a study by [Cornelissen 1984]. Figure 13 shows that the maximum strength, regardless of the water/cement ratio occurs when a No. 4 Sieve was used.

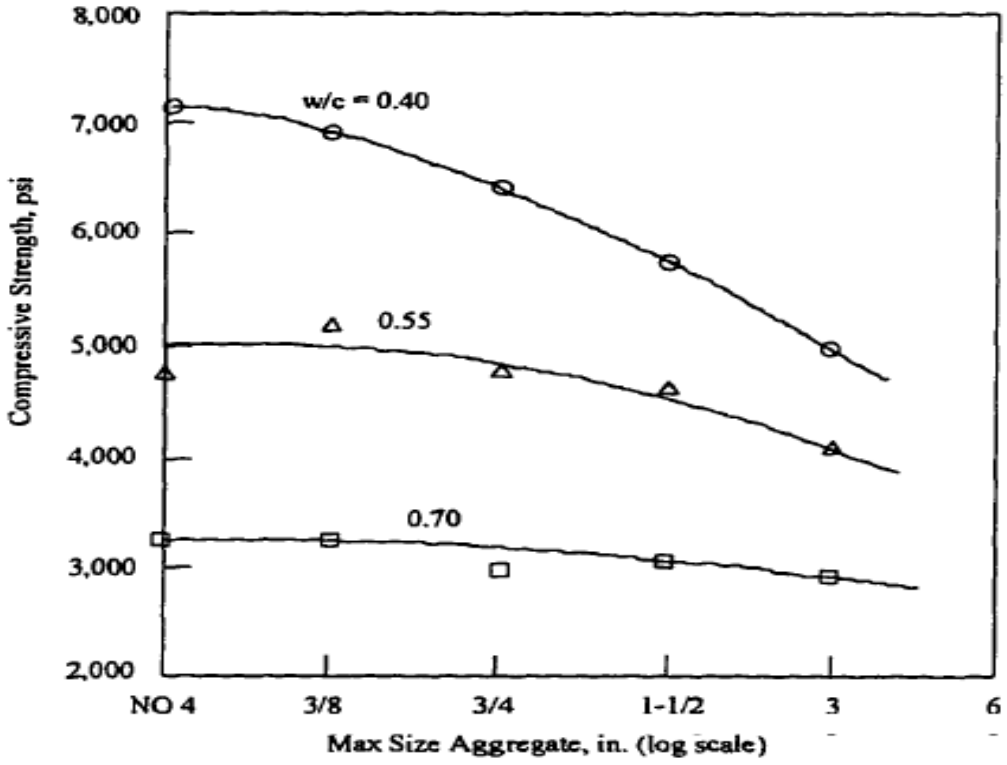

Figure 13 - Influence of the aggregate size and the water/cement ratio on concrete strength [Cornelissen 1984]

The material in the pre-prepared mix was very dry, such that there was likely a fairly uniform water content in this material relative to the standard batch plant where materials are typically exposed to the elements and a broad range of humidities. This partly explains the narrow range of compressive strengths that were presented in Table 1.To each batch the author added a water weight of 13.9% of the total mix weight, which was an amount found to provide a workable mix with segregation. The amount of water added to each batch was precisely controlled by the use of a laboratory scale. This was based on testing that occurred in the first three specimens that were cast

3.5 Curing Process

Each specimen was allowed 24 hours to develop sufficient strength before being removed from the molds. They were then placed in a room temperature environment of approximately 72 degrees Fahrenheit in wet towels on all four sides of the specimen. The specimens were then sealed with a non-permeable plastic covering to keep the moisture content consistent. See Figure 14 and Figure 15 for the towel and plastic seal setups.

Figure 14 - Curing specimens

Figure 15 - Plastic seal over curing specimens

The specimens were left to cure for six days and then the plastic and towels were removed to allow the specimens to dry one day prior to testing.

3.6 Test Procedure and Instron 8501

The testing of these concrete specimens was carried out using an Instron 8501. The Instron 8501 is a servo-hydraulic fatigue testing machine that is capable of testing tensile strength, compressive strength, tensile fatigue, compressive fatigue and a combination of tensile/compressive fatigue. The machine is rated up to 22 kips, which was much larger than the loads applied in this study that were less than 4 kips.

Figure 16 – Instron 8501 testing setup

The Instron 8501 was controlled using Bluehill 2 software. This software allowed the user a broad range of testing abilities for tensile strength and tensile fatigue testing. Specifically, it allowed the author to write his own loading programs to test each set of specimens at varying stress levels and frequencies. One of the sample loading sequences can be seen in Figure 17.

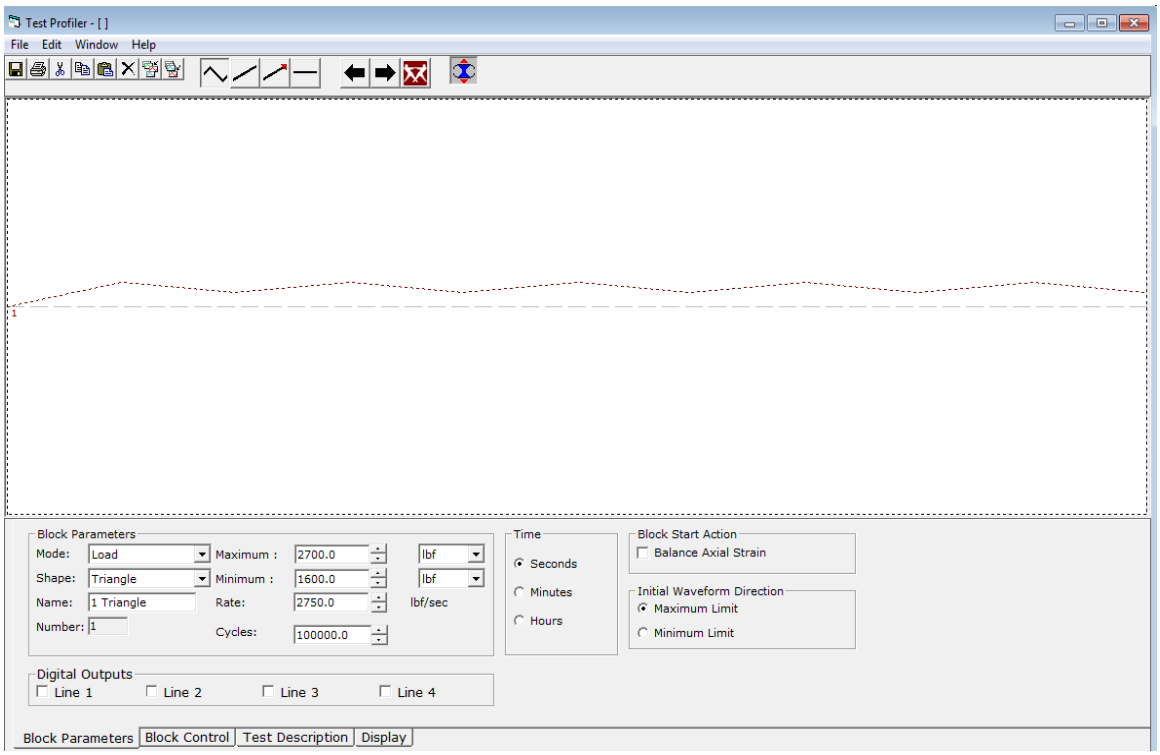

Figure 17 – Bluehill 2 cyclic loading pattern

Each test was continued until a pre-coded stop command was met. In the case of all of these tests, it was when the tensile deformation reached 0.5”. Once the concrete cracked, the machine would continue to separate the specimen as there was nothing holding it together. The stop command was met at every failure, which allowed tests to be run continuously.

The Instron had difficulty testing at high frequencies so a frequency less than 1 Hz was used. The tests were eventually carried out at 0.75 Hz, which was discovered to be the limit of this machine for this setup. It also had difficulty outputting all the data in one run so the machine would have to be stopped every 14,000 cycles if the specimen continued for that long without failure.

Chapter 4. Experimental Observations and Data Analysis

4.1 Experimental Observations

4.1.1 Failure Mechanism Modes

The specimens made in this experiment were, to the best of the author's knowledge, the first of their kind. This is considered likely because no current data was found in the literature for the types of tests conducted by the author. It was hypothesized in this project that there would be two major failure types before the experiments began. These two types were: failure in the unreinforced section and failure at the steel-concrete connection. The unreinforced failure was an obvious prediction as concrete is weak in tension. This was the ideal failure to occur because it would mean that the concrete had reached its capacity and failed without any other forces being induced.

Figure 18 – Failure plane in unreinforced section

Failure at the steel-concrete connection was another possible failure mechanism as there would possibly be a weakened plane due to the steel terminating in the concrete at that point. In addition, if the specimen was not perfectly in uniaxial tension there would be additional stress concentration at that connection.

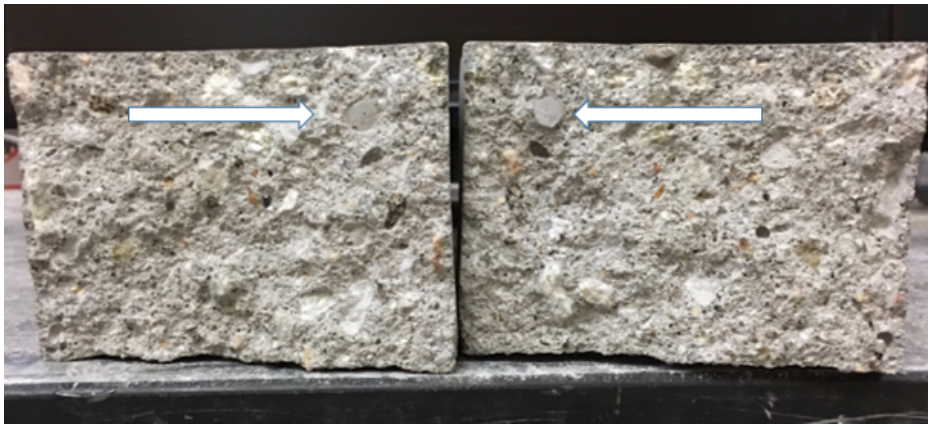

Figure 19 – Failure at steel-concrete plane. The right arrow indicates rebar protruding from concrete, the left arrow indicates where the steel left a circular mark in the concrete.

While these two failure modes both occurred, there were additional failure types that happened and need to be documented and discussed.

The two additional types of failure were caused by the rebar detaching from the concrete and a failure in between the two longer rebar connections. The rebar detaching was caused by a misalignment of the rebar cast into the concrete. The rebar was then not able to fit into the holes displayed in Figure 11 on the metal plate. These specimens were still tested, but because the rebar had to be forced into the holes, it weakened the connection of the steel with the concrete and resulted in very early failure of the specimen. These defective specimens were noted in Table 2 as having difficulty attaching the cast rebar into the metal plates. This can be seen in specimens #5, #10 and #15. The rebar detaching was not an expected failure because it was based on the assumption that the mold would be correct for each sample. Originally, the molds were perfectly aligned so the rebar would slide easily into the metal testing plate, but as the wood began to warp, the holes changed angles and made it more difficult to ensure the correct alignment. This was fixed

in specimens #16 through #20. The second failure that was unexpected was similar to the specimen failing at the concrete-steel connection, but instead of failing in a straight line, it failed between the two longer rebar rods.

Figure 20 shows the concave of the failure plane in Specimen #8.

Figure 21 - Failure plane between the two longer rebar

Although this failure seemed the least likely to occur because of the odd shaped failure plane, reasons for this failure could have been poor mixing between the rebar as the concrete was poured, which resulted in air pockets or because the stress caused by misaligned rebar created a weak point in the concrete.

Table 2 – Specimen loading pattern, cycles until failure and failure mechanism

Specimen Number	Number of Cycles Until Failure	Failure Mechanism
1	NA	Unreinforced section
2	412	Unreinforced section
3	3439	Steel-concrete plane
4	199	Failure between rebar
5	0	Rebar separation
6	6	Unreinforced section
7	22063	Steel-concrete plane
8	24369	Unreinforced section
9	2	Unreinforced section
10	2	Rebar separation
11	84	Unreinforced section
12	75	Failure between rebar
13	27450	Steel-concrete plane
14	604	Steel-concrete plane
15	11	Rebar separation
16	3620	Steel-concrete plane
17	34	Steel-concrete plane
18	52426	Unreinforced section
19	9180	Unreinforced section
20	15102	Unreinforced section

Table 3 – Comments about specimen construction

Specimen Number	Comments About Specimen Construction
1	Some spalling
2	Some spalling, strain gauge resin could influence failure location
3	Some spalling
4	Good specimen
5	Difficulty attaching metal plates
6	Good specimen
7	Good specimen
8	Good specimen
9	Very bent, will most likely fail early
10	Slightly bent, difficulty attaching metal plate, will most likely fail early
11	Good specimen
12	Good specimen
13	Good specimen
14	Good specimen

15	Difficulty attaching metal plate
16	Good specimen
17	Good specimen
18	Good specimen
19	Good specimen
20	Good specimen

4.1.2 Failure Mechanism Results

There were 9 failures classified to be in the unreinforced mode (45% of the total number of tests), 6 steel-concrete plan failures (30% of total), 2 tests between rebar (10% of total), and 3 that had rebar separation (15% of total). There is no clear connection between failure located in the unreinforced portion, steel-concrete plane, and between the rebar in terms of number of cycles. When plotted on the S-N curve each failure mechanism occurs throughout the log scale at varying amounts, with no pattern forming. The one clear failure type that resulted in a specific amount of cycles was failure by rebar separation. Failure in this manner was expected due to the significant stress concentrations and the inability of the concrete to withstand any sort of unbalanced load.

4.1.3 S-N Curves from Test Specimens

The S-N curve y-axis was the stress applied over the cracking capacity of the concrete in pure tension. The only other test similar to this [Cornelissen 1982] used the cracking capacity of 500 pure tensile tests as the f_r of the test. The author in this research employed the commonly used $4\sqrt{f'_c}$ as the cracking capacity of uniaxial tension as this has been thoroughly documented and is regarded as a fair assumption. The stresses applied were based upon that value and those are the data points displayed on the following S-N curves. The following S-N curves were plotted with the upper loading

stress, the mean, and the lower loading stress so the reader can view the range and the mean loading value.

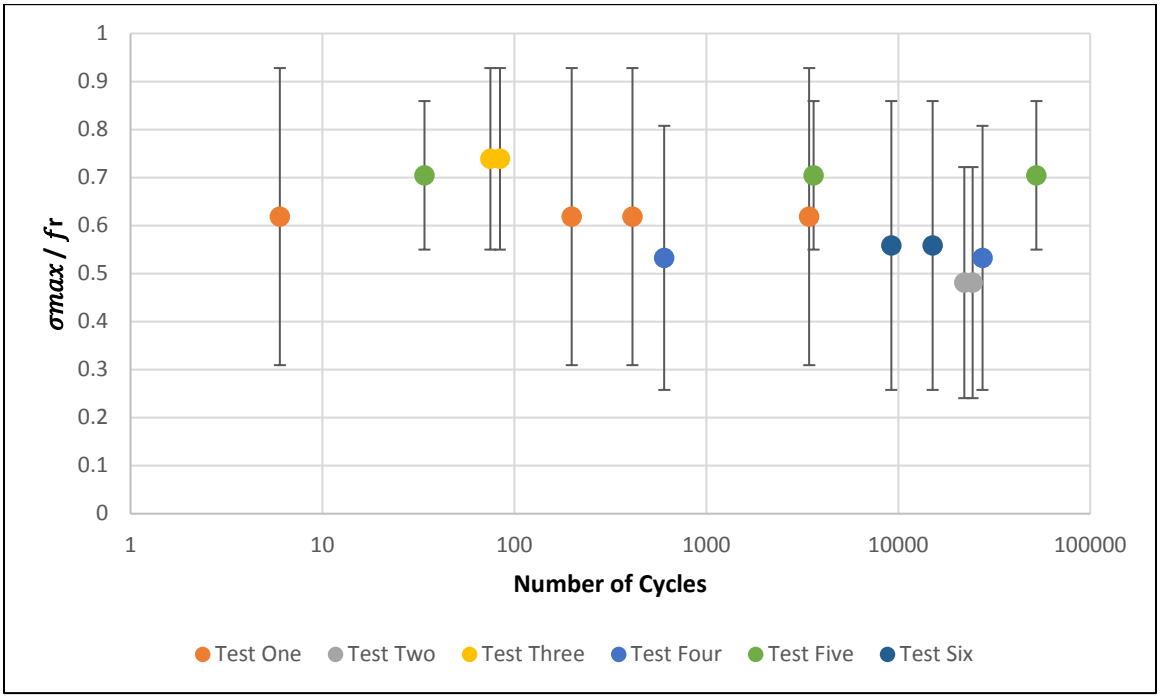

Figure 22 - S-N curve of tested specimen dataset

Figure 21 shows the results of the six tests conducted in this experiment. Each test involved a different loading pattern applied. There were 20 specimens tested in this thesis, but specimens #1, #5, #9, #10 and #15 were not included in the results. Specimen #1 was tested to failure in continuous loading to test the maximum stress a specimen could withstand and to see if it was close to the predicted $4\sqrt{f'_c}$ the stresses deemed acceptable. This is displayed in Table 4.

Table 4 - Predicted stress vs tested stress

	Stress (psi)
Specimen #1	303.04
$4\sqrt{f'_c}$	252.98

Specimens #5, #10, #15 all had failures of rebar separating from the sample and were deemed to be unfit for inclusion in the dataset to be analyzed. Specimen #9 failed before five cycles were met and therefore was deemed unfit for inclusion in the dataset.

There was a fair amount of variability in the data gathered as expected due to natural variability in the static tensile strength of concrete. The data showed some clear patterns. Two patterns were:

- increasing the maximum load decreased the number of cycles until failure
- increasing the range at which the cycles were tested decreased the number of cycles until failure.

Averaging data points based upon the load at which they were tested would allow for better analyses of the specimens and would mitigate the scatter associated with viewing a graph of independent tests.

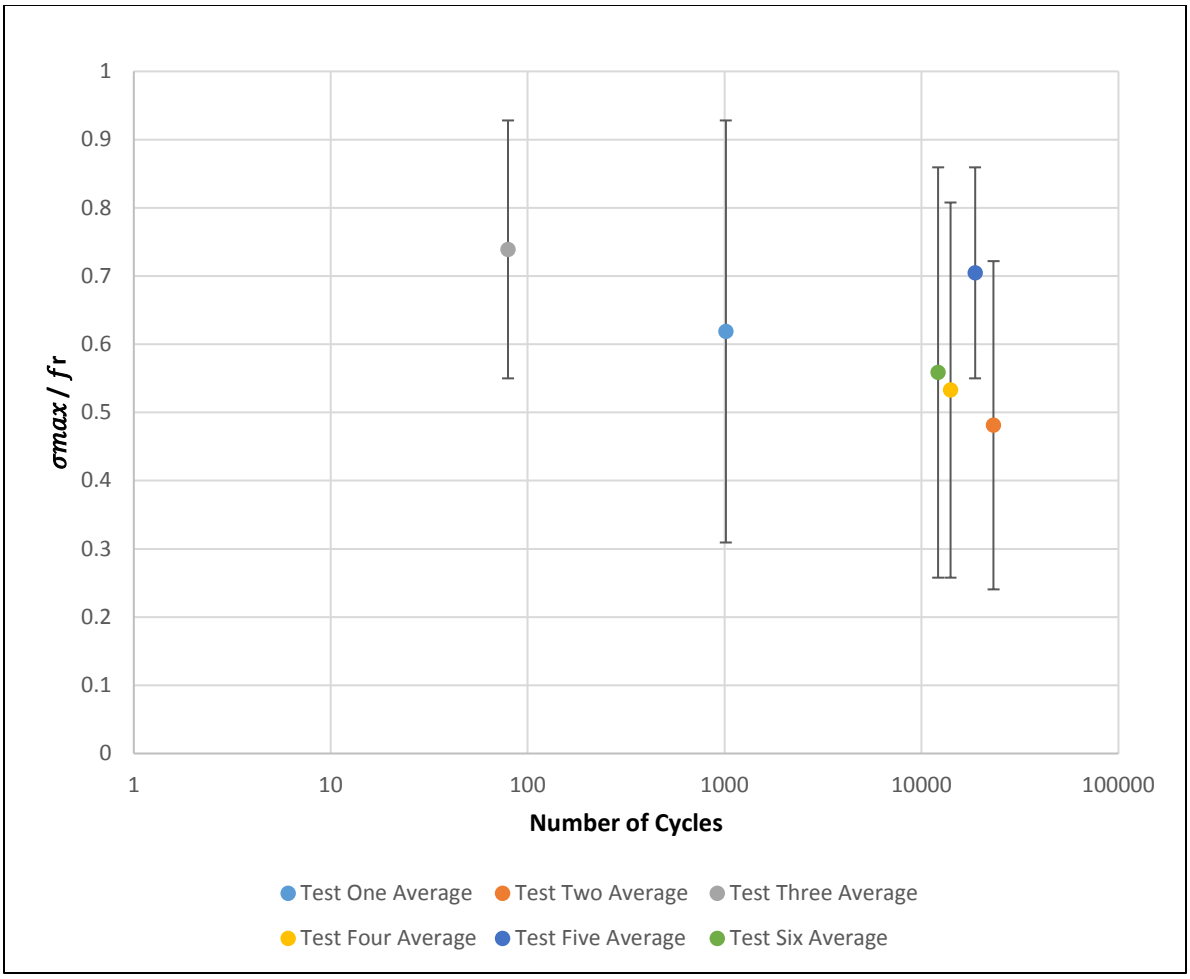

Figure 23 - S-N curve of average based on stress applied to specimens

Averaging the collected data in this thesis showed a clear improvement in predicted response, especially when tests Two, Four, Five, and Six are compared.

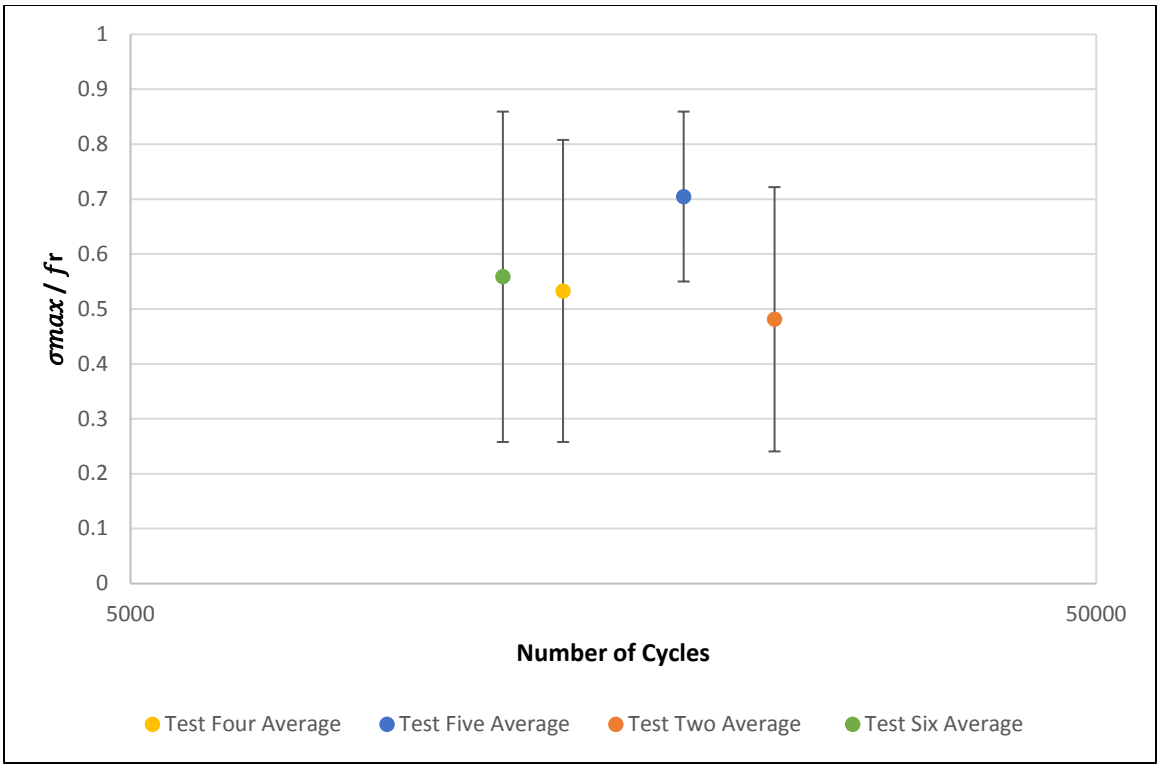

Figure 24 - S-N curve of averaged data based on stress applied to specimens between 5000 and 50000 cycles

As the maximum stress ratio was reduced in Test Six to Test Four from 0.86 to 0.81, an increase in the number of cycles to failure from 12,147 to 14,027 was observed, respectively. Additionally, when the maximum stress ratio was reduced further in Test Two to 0.72, the average number of cycles to failure further increased to 23,216.

This dataset subset also shows that when two tests had the same maximum stress ratio and the range of loading was reduced the number of cycles to failure increased. The range of loading decreased from Test Six to Test Five from 0.6 to 0.31 and the number of cycles to failure increased by 12,147 to 18,693, respectively.

The averages from tests Three and One do not support the observations just mentioned. There was a wide range of variability in these experiments and as the concrete was tested closer to its maximum capacity, as it is in these two tests, any weaknesses in the concrete were exposed more quickly, which could lead to more variability in the graph. The positive takeaway from these two tests was that they were tested at the highest stresses in this thesis and failed earlier than the tests tested at lower stresses, which is consistent with predictions made by the research team and previous documentation by [Cornelissen 1982, 1984, 1985].

4.1.4 Synthesis of Cornelissen 1982 Data

The only other project that was found in which a similar form of experimental testing was conducted in the work of the Technical University at Delft (TU-Delft) in the Netherlands in the [Cornelissen 1982, 1984, 1985] reports. A dataset was obtained from [Cornelissen 1982] to compare with the dataset in this thesis. The dataset included 87 specimens tested in uniaxial tensile concrete fatigue. Instead of using threaded rods into the specimen, the research team at TU-Delft used an epoxy resin to attach to the testing device.

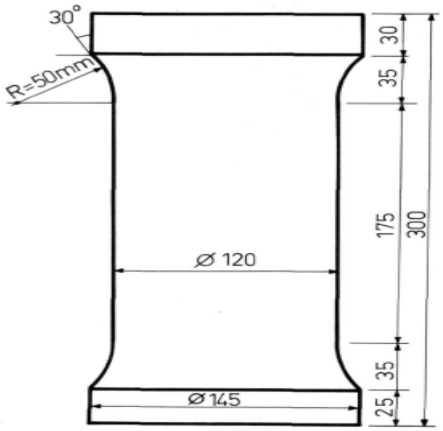

Figure 25- Specimen used in [Cornelissen 1982] test

In order to use the TU-Delft research in this thesis, the 87-specimen database was reduced to 61 specimens upon removing specimens that failed to break before 10^5 cycles. The author decided to do this as this thesis is only interested in high stress, low cycle fatigue and no points collected from this thesis exceeded 10^5 cycles. For a complete list of [Cornelissen 1982] specimens see Appendix B.

These tests were not a match in specimen size, curing length, water content, or loading frequency, but as this is the only dataset found the two would be normalized based on their maximum stress capacity to stress applied in testing and plotted on an S-N curve to be compared.

4.1.5 S-N Curves Comparing Thesis Test Specimens with Cornelissen 1982 Data

Although these tests were carried out over 30 years apart using a plethora of different testing conditions, when the stress values were normalized and plotted with the [Cornelissen 1982] values there was a correlation between the two. It is difficult to understand possible trends from all 76 combined specimens so a graph with the averages was created.

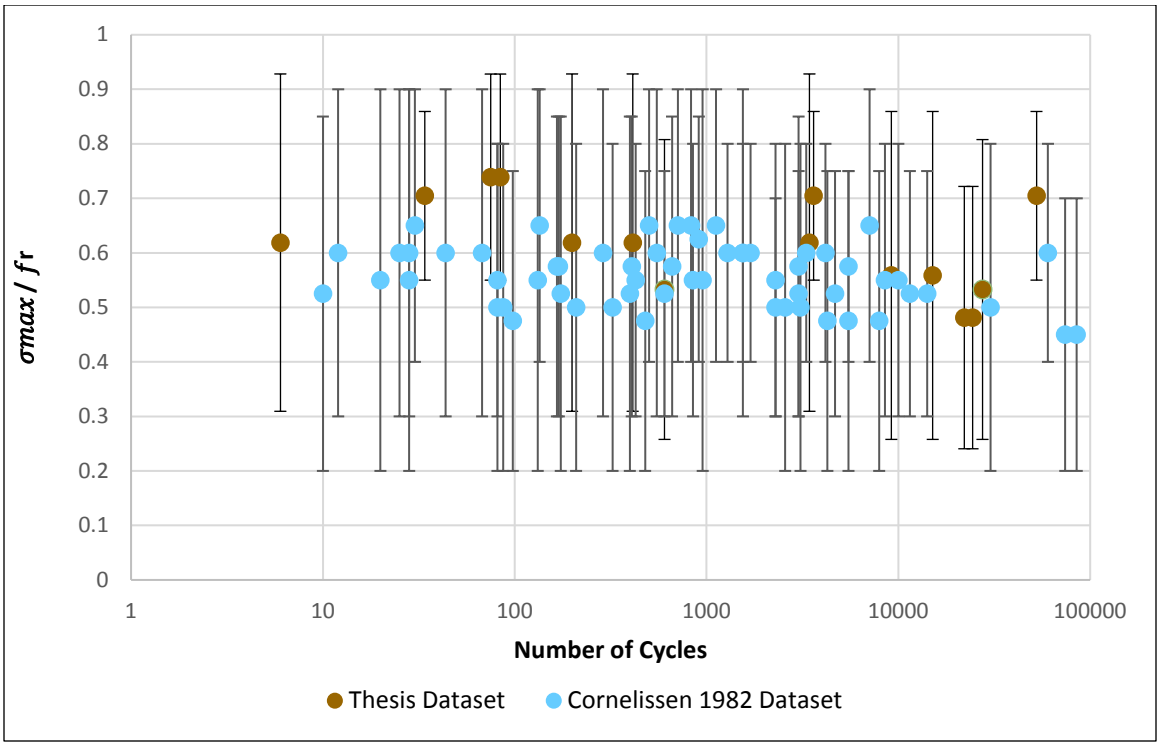

Figure 26 - S-N curve of combined datasets

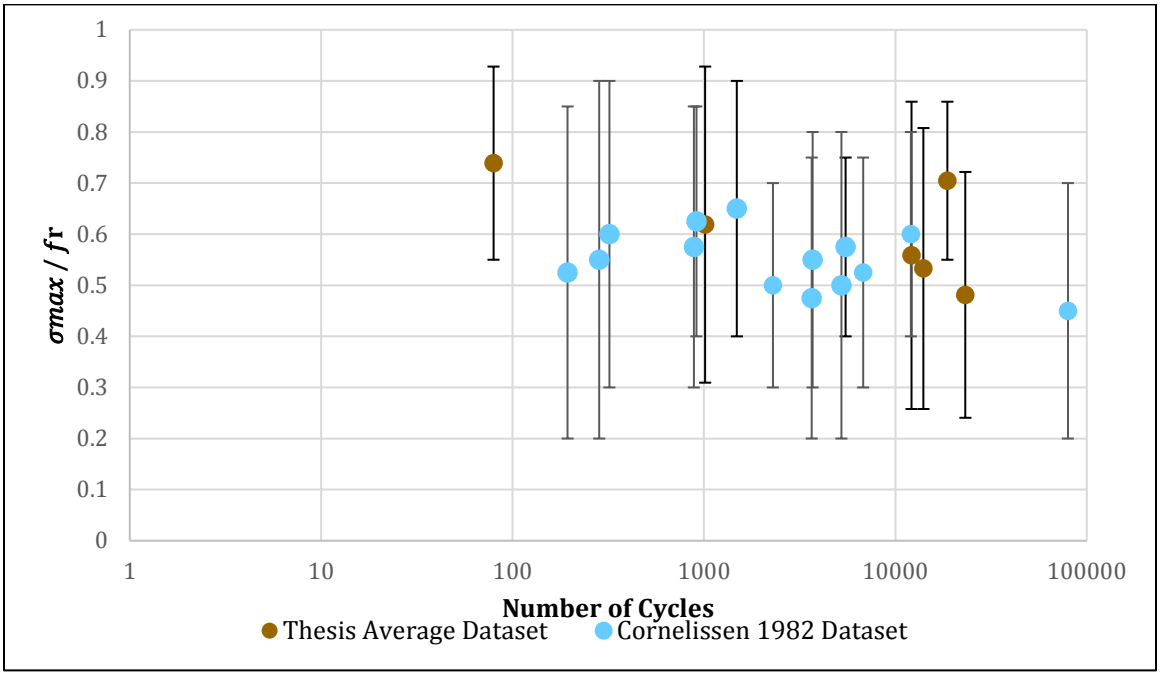

Figure 27 - S-N curve of combined averaged data based on stress applied to specimens

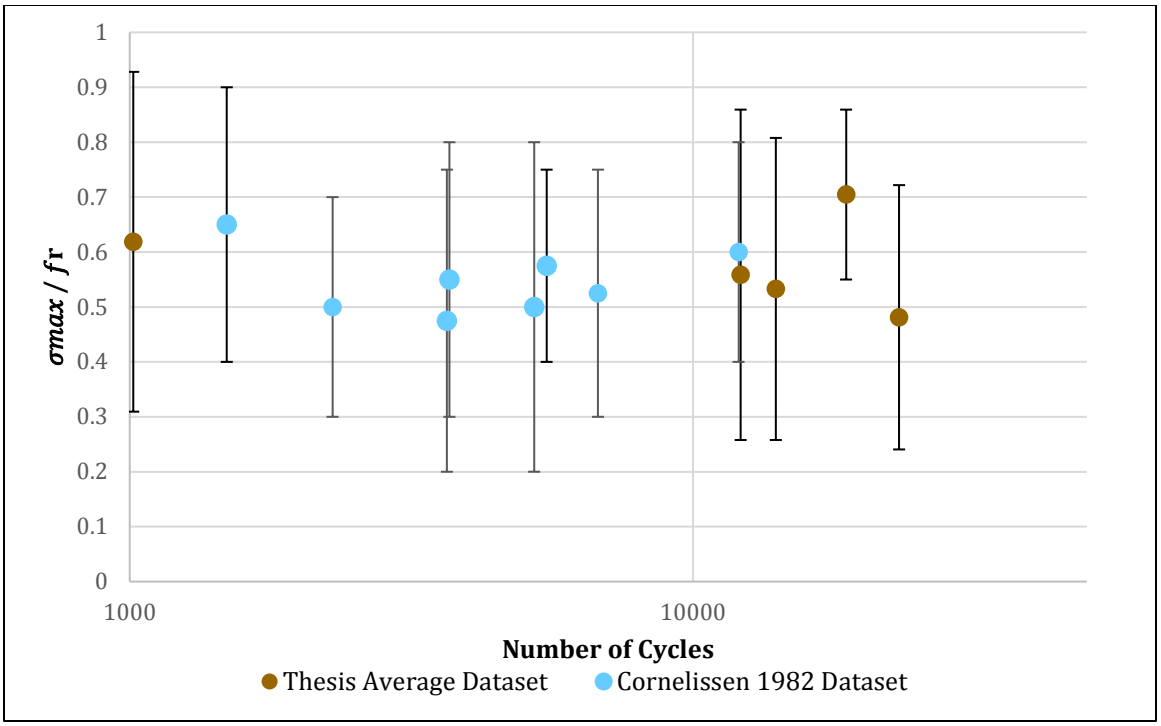

Figure 28 - S-N curve of combined averaged data based on stress applied to specimens from 1000 to 50000 cycles

The data from the testing conducted in the Tufts University study appears to validate the [Cornelissen 1982] report and that the tests at Tufts were properly done as the datasets are comparable in stresses applied and number of cycles until failure.

4.2 Validation of Uniaxial Testing

In the second specimen tested, four strain gauges (SG) were attached at the middle of the specimen to see if the strain distributions were even throughout the test. This test was done in order to ensure that the sample was in pure uniaxial tension. The testing was done using a Micro-Measurements Model P3 Strain Indicator and Recorder. The Micro-Measurements Model P3 Strain Indicator and Recorder is a mobile recording device that allows for continuous recording as a test is going on. This allowed the specimen to be

strain gauged and tested in close proximity. The only downside of this testing device was that it could only record at a frequency of one reading per second, which meant that the peak values could be missed at some points during the testing. To counteract this slow data acquisition time, the loading on the specimen was done slowly to allow the P3 to capture as many data points along the cycle as possible.

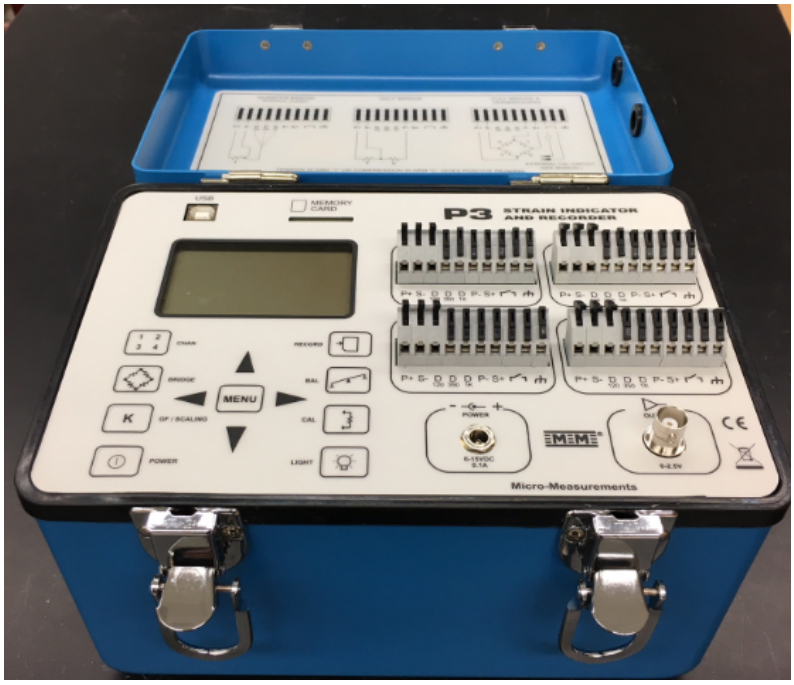

Figure 29 - Micro-Measurements Model P3 Strain Indicator and Recorder

The strain gauge layout on the specimen can be seen in Figure 29 and Figure 30 below.

Figure 30 - # 1, 2, 3 strain gauge layout

Figure 31 - #2, 3, 4 strain gauge layout

SG #1 and SG#4 should have identical strains for each cycle as they are located on the same plane of the concrete. The same should be true of SG #2 and SG #3. The results of the strain gauges can be seen in Figure 31 and 32.

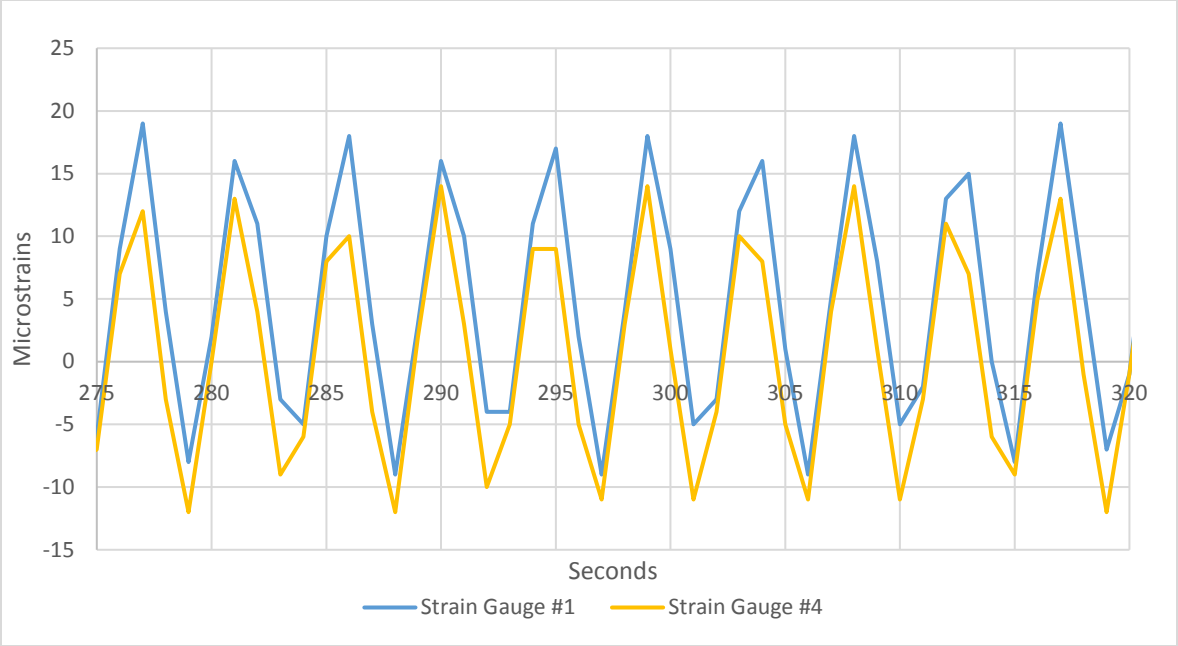

Figure 32 – Strain gauge #1 and #4 outputs

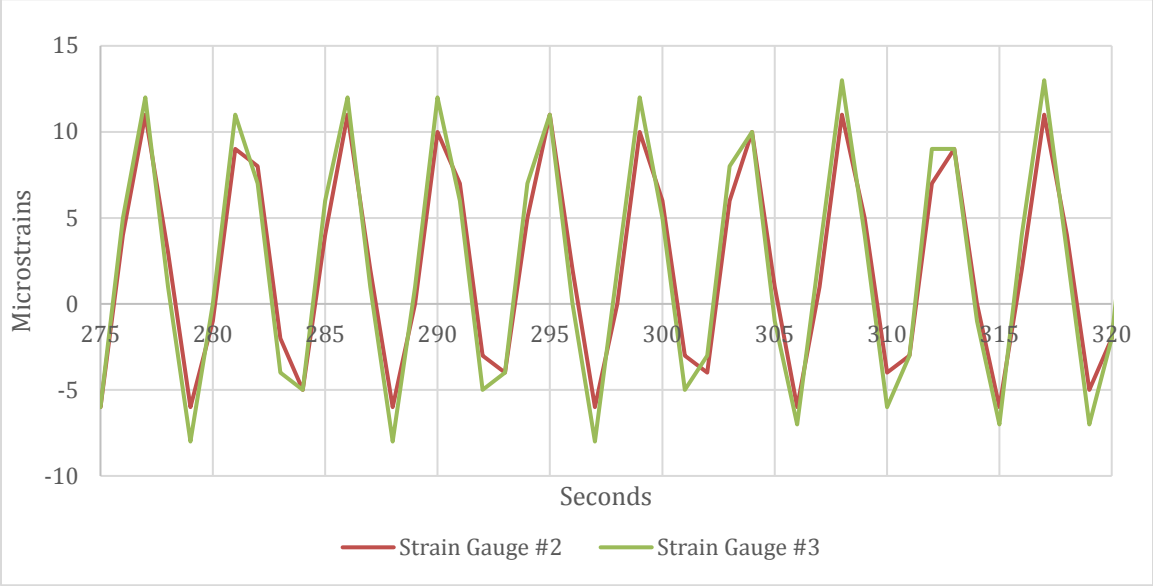

Figure 33 - Strain gauge #2 and #3 outputs

These results present that the strains in SG #1 and SG #4 were very similar in magnitude per each cycle. The same can be observed in SG #2 and SG#3. This helps to substantiate that the test was in pure axial tension. The question that could arise from the range being

nearly identical, but the maximum and minimum values not being identical, could be answered by the fact that the system was zeroed before the loading started on the sample. There could have been sudden deformations once the load was applied and zeroing after initial loading would have resulted in nearly identical strain maximum and minimum.

Chapter 5. Conclusions and Suggested Future Work

5.1 Conclusions

The aim of this research was to investigate uniaxial tensile concrete fatigue. A test setup was developed and the number of cycles to failure was recorded. The conclusions of this thesis are based upon the data and observations included in Chapter 4 and they are:

- 15 concrete specimens were tested in high stress uniaxial tensile fatigue and added to a previous database of 61 specimens, therefore creating a more robust dataset for future analysis.
- The results show that concrete was affected by both the maximum stress applied and the range of the stress applied. As the stress increased, the number of cycles to failure decreased and similarly, as the stress range increased, the number of cycles until failure decreased.
- The specimens were confirmed to be in pure uniaxial tension by strain gauging Specimen #2 and comparing the strains at each location.
- These tests were compared with research done by [Cornelissen 1982] and the data suggested a strong correlation between the two datasets, therefore validating the authenticity of the previous test and this current research.

5.2 Future Work

This thesis has started to research uniaxial tensile concrete fatigue as it pertains to offshore wind turbines, but there is still significant research to be done. This same research could be taken to the next level through more specimen testing. Instead of just

27 specimens, hundreds could paint a better picture of tensile fatigue testing in plain concrete. Because there is a small amount of research currently in the field, simply adding more data points using a similar testing setup would be beneficial. This thesis does not investigate the effects of the specimen being exposed to both tension and compression in loading, but Cornelissen did investigate it. Confirming their results or simply adding more data to the field would be another avenue of research. Examining high-cycle uniaxial fatigue loading using these same specimens on a testing machine that is capable of loading multiple cycles per second to avoid the long testing time, is another possible avenue for future research. Using different sized specimens, testing different mixes, testing different aggregates, different w/c ratios, reinforced specimens, effects of saltwater on fatigue are examples of other under researched areas in the field that could contribute to advancing our understanding of the fatigue performance of concrete and its suitability for use in foundations and towers of offshore wind turbines.

Chapter 6. References

ABS. (2011). *Design Standards for Offshore Wind Farms*. Washington, D.C.: American Bureau of Shipping.

ACI Committee 215: Fatigue of Concrete Structures, (Editor Shah, S.P.), American Concrete Institute, Publication SP-75, Detroit 1982.

"Bill H.4568 189th (2015 - 2016)." *Bill H.4568*. Web. 16 May 2017. <https://malegislature.gov/Bills/189/House/H4568>.

Cornelissen, H.A.W., "Fatigue Failure of Concrete in Tension," Heron, Vol. 29, No. 4, 1984.

Cornelissen, H.A.W., and Siemes, A.J.M., "Plain Concrete under Sustained Tensile or Tensile and Compressive Fatigue Loadings," in Proceedings BOSS Conference, Elsevier, 1985, pp. 487-498.

Cornelissen, H.A.W., and Timmers, G, "Fatigue of plain concrete in uniaxial tension and in alternating tension-compression," Delft University, 1982.

Fields, R. (2008). "The Importance of Standards in Engineering." Presentation to ASTM International Committee D30 on Composite Materials. Lockheed Martin Missiles and Fire Control.

Gilman, Patrick, Ben Maurer, and Luke Feinberg. "National Offshore Wind Strategy." N.p., n.d. Web. <https://www.boem.gov/National-Offshore-Wind-Strategy/>.

Hawkins N.M., and Shah S.P. American Concrete Institute Considerations for Fatigue. IABSE Colloqium, "Fatigue of Steel and Concrete Structures," Lousanne, March 1982, Proceedings IABSE Reports, Vol. 37, Zurich, 1982, pp. 41-50.

Henderson, A. R., Morgan, C. S., Smith, B., Sørensen, H. C., Barthelmie, R. J., and Boesmans, B., "Offshore Wind Energy in Europe — A Review of the State-of-the-Art," *Wind Energy*, Vol. 6, No. 1, February 2003, pp. 35–52.

Hordijk, D.A., "Local Approach to Fatigue of Concrete," Ph.D. dissertation, Delft University, 1991.

Hsu, T.T.C. "*Fatigue of plain concrete."* Proceeding of the ACI, Vol. 78, 1981.

Joly D (1898) La resistance et l, ‘‘elasticite des’’ ciments Portland. Ann Pons Chaussees 16(7):198–244

Kolias, S. and Williams, R.I.T. " *Cement -bound Road Materials: Strength and Elastic Properties Measured in the laboratory."* TRRL Report No. 334, 1978.

Miner, M., 1945. Cumulative Damage in Fatigue. J. Appl. Mech. 12, 159–163.
Morris, A.D. and Garrett, G.G. " *A Comparative Study O f the Static and Fatigue Behavior o f Plain and Steel Fiber Reinforced Motor in Compression and Direct Tension."* Int.

Murdock, John W. "A Critical Review of Research on Fatigue of Plain Concrete." *University of Illinois Bulletin* 62.62 (2007).

Musial, W., Butterfield, S., and Boone, A., "Feasibility of Floating Platform Systems for Wind Turbines," *A Collection of the 2004 ASME Wind Energy Symposium Technical Papers Presented at the 42nd AIAA Aerospace Sciences Meeting and Exhibit, 5–7 January 2004, Reno Nevada, USA*, New York: American Institute of Aeronautics and Astronautics, Inc. (AIAA) and American Society of Mechanical Engineers (ASME), January 2004, pp. 476–486, NREL/CP-500-36504, Golden, CO: National Renewable Energy Laboratory.

Musial, W. and Ram. B. (2010). *Large-Scale Offshore Wind Power in the United States: Assessment of Opportunities and Barriers.* National Renewable Energy Laboratory, Golden, Colo. NREL/TP-500-40745. http://www.nrel.gov/wind/pdfs/40745.pdf.

"Offshore Wind Turbine Foundations- Current & Future Prototypes." *OffshoreWind.net*. N.p., 11 Jan. 2016. Web. 09 May 2017. <http://offshorewind.net/offshore-wind-turbine-foundations-current-future-prototypes/>.

Paris, P.C., and Erdogan, F., "A Critical Analysis of Crack Propagation Laws," Journal of Basic Engineering, Transactions ASME, Series D 85, 1963, pp. 528-534.

Raithby, K. D. Some flexural fatigue properties of concrete-effects of age and methods of curing. *First Australian Conference on Engineering Materials, University of New South Wales, 26-28 August 1974.* Kensington, University of New South Wales, 1974. Pp. 211-229

RILEM Committee 36-RDL, "Long Term Random Dynamic Loading of Concrete Structures", RILEM Materials and Structures, Vol. 17, No. 97, 1984, pp. 1-28.

Schlossberg, Tatiana. "America's First Offshore Wind Farm Spins to Life." *The New York Times*. The New York Times, 14 Dec. 2016. Web. 09 May 2017. <https://www.nytimes.com/2016/12/14/science/wind-power-block-island.html?_r=0>.

Shah,S.P., and Chandra, S., "Fracture of Concrete Subjected to Cyclic and Sustained Loading," Journal of American Concrete Institute, Vol. 67, No. 9,1970, pp. 816-825.

Sirnivas, S., W. Musial, B. Bailey, and M. Filippelli. "Assessment of Offshore Wind System Design, Safety, and Operation Standards." (2014): n. pag. Web.

Tepfers, R. Tensile fatigue strength of plain concrete. *Journal of the American Concrete Institute. Proceedings* Vol. 76, No. 8. August 1979. pp 919-933

Valamanesh, V., A.T. Myers, and S.R. Arwade. *Multivariate Analysis of Extreme Metocean Conditions for Offshore Wind Turbines*. N.p., n.d. Web. 10 May 2017. <http://www.sciencedirect.com/science/article/pii/S0167473015000296>.

Van Ornum, J.L., "The Fatigue of Concrete," Transactions, ASCE, Vol. 58, 1907, pp. 294-320.

Watson, G., et al, "A Framework for Offshore Wind Energy Development in the United States," *Massachusetts Technology Collaborative (MTC)* [online publication], URL: http://www.mtpc.org/offshore/final_09_20.pdf, [cited 17 November 2005].

Wave Information Studies. US Army Corps of Engineers, Web. 05 June 2017. <http://wis.usace.army.mil/hindcasts.html>.

Chapter 7. Appendices

Appendix A

Figure 34 - Specimen #1 failure plane view

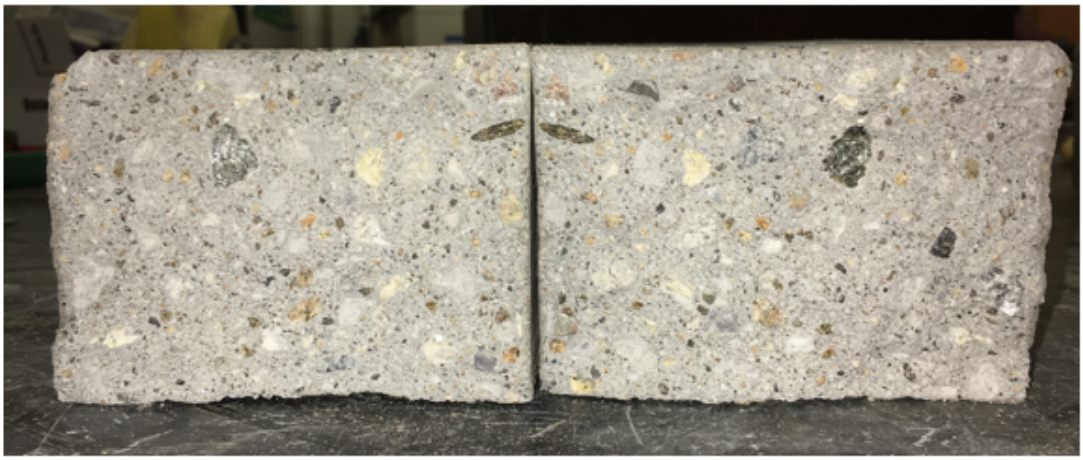

Figure 35 - Specimen #1 failure cross-section

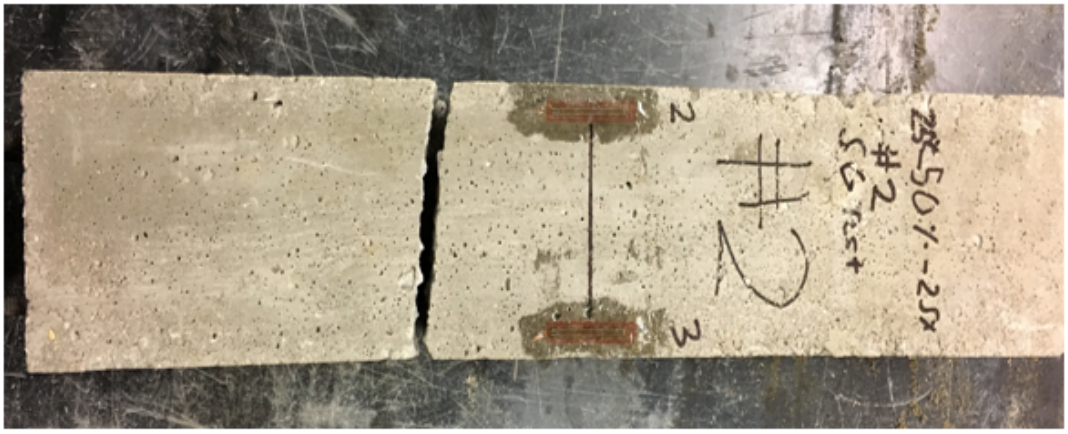

Figure 36 - Specimen #2 failure plan view

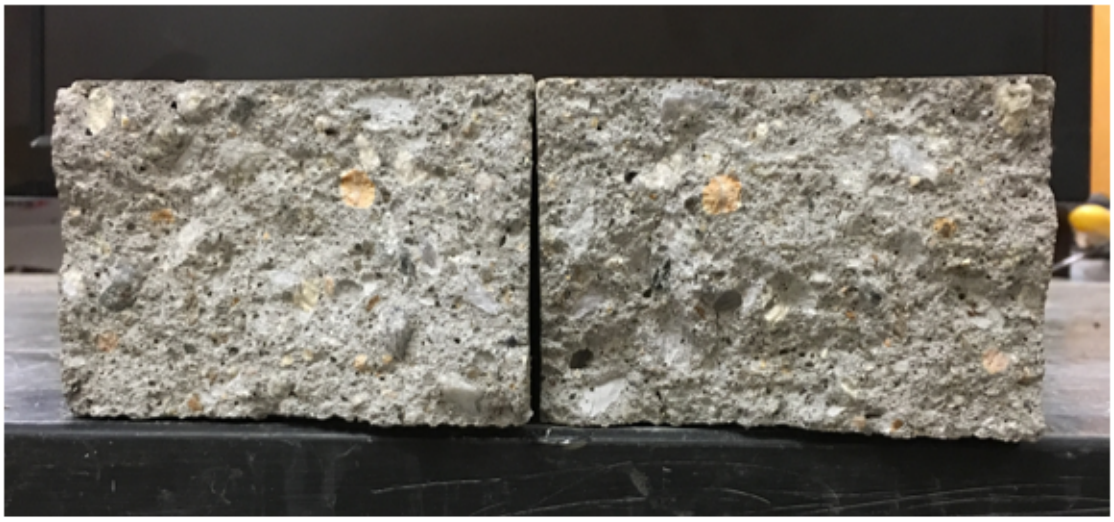

Figure 37 - Specimen #2 failure cross-section

Figure 38 - Specimen #3 failure plan view

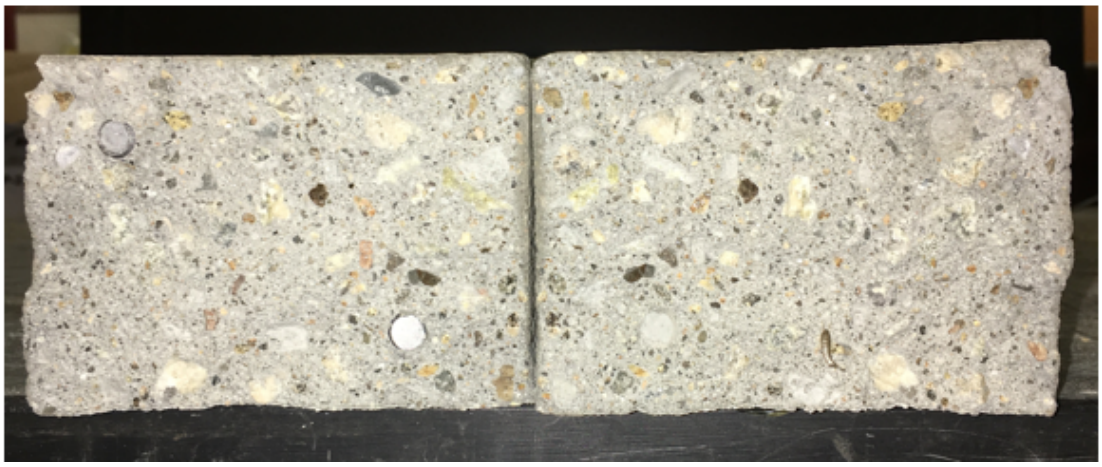

Figure 39 - Specimen #3 failure cross-section

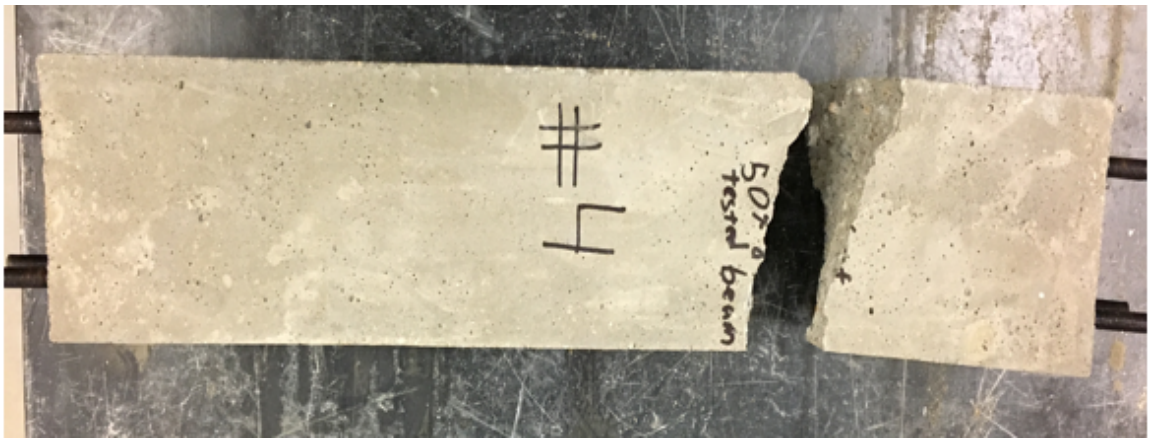

Figure 40 - Specimen #4 failure plan view

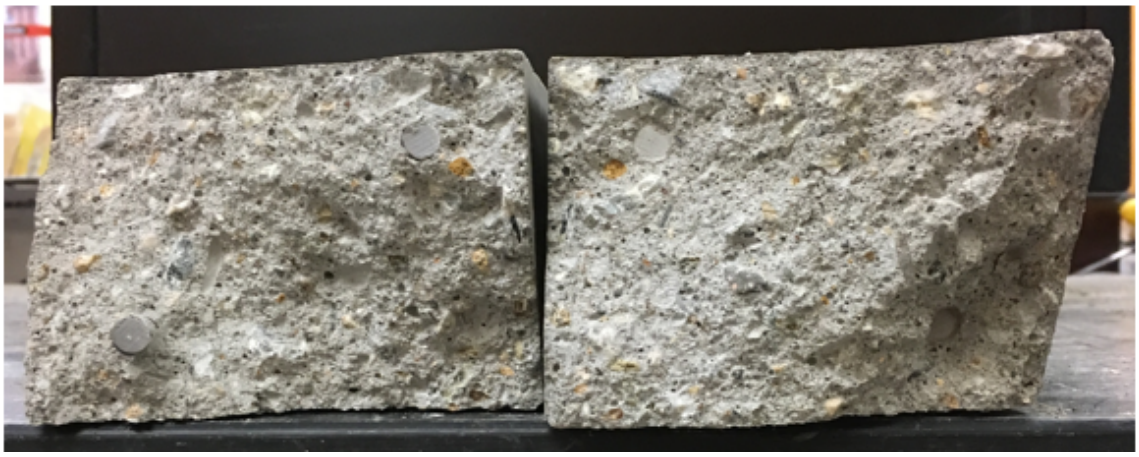

Figure 41 - Specimen #4 failure cross-section

Figure 42 - Specimen #5 failure plan view

Figure 43 - Specimen #5 failure cross-section

Figure 44 – Specimen #5 surface cracking

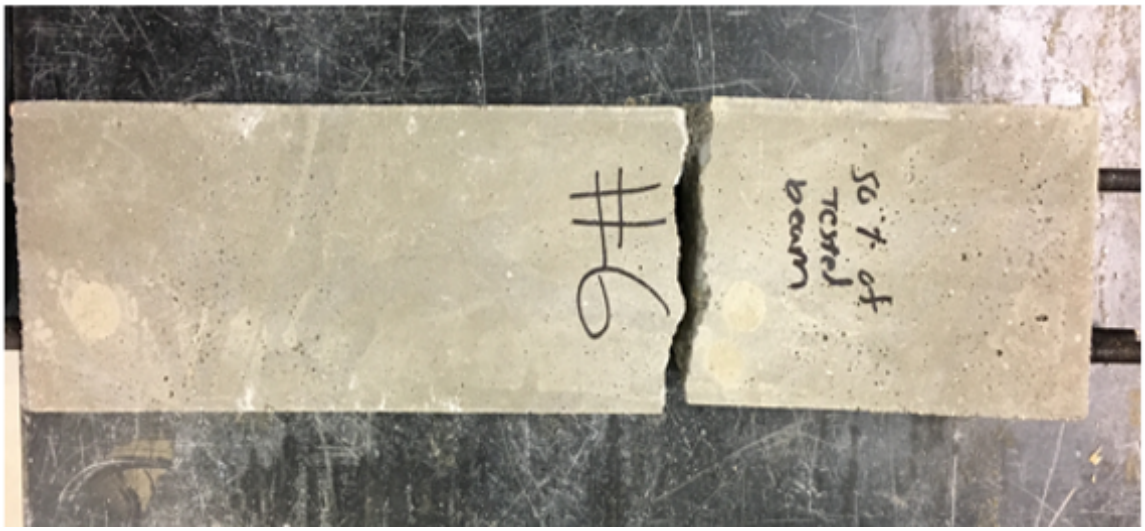

Figure 45 - Specimen #6 failure plan view

Figure 46 - Specimen #6 failure cross-section

Figure 47 - Specimen #7 failure plan view

Figure 48 - Specimen #7 failure cross-section

Figure 49 - Specimen #8 failure plan view

Figure 50 - Specimen #8 failure cross-section

Figure 51 - Specimen #9 failure plan view

Figure 52 - Specimen #9 failure cross-section

Figure 53 - Specimen #10 failure plan view

Figure 54 - Specimen #10 failure cross-section

Figure 55 - Specimen #11 failure plan view

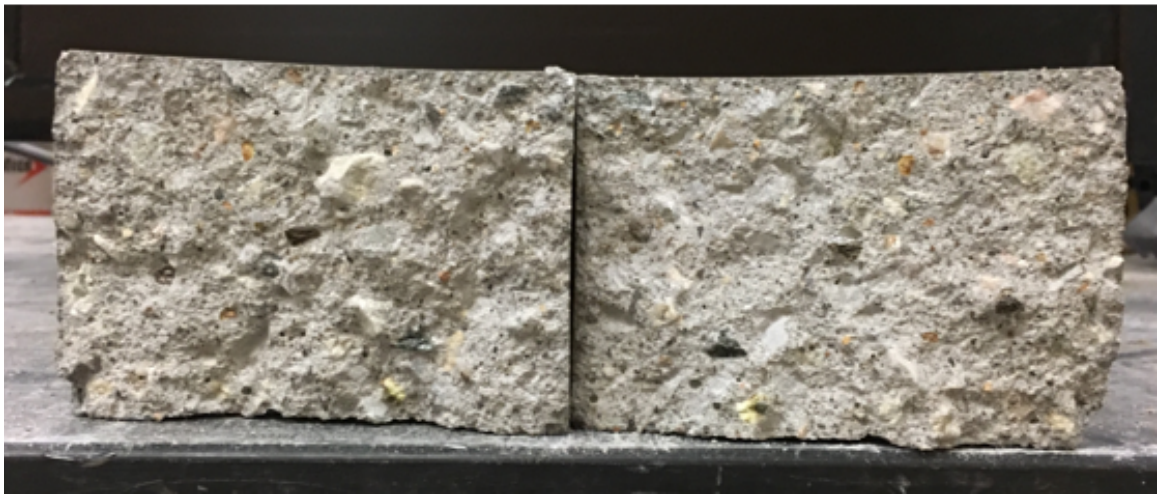

Figure 56 - Specimen #11 failure cross-section

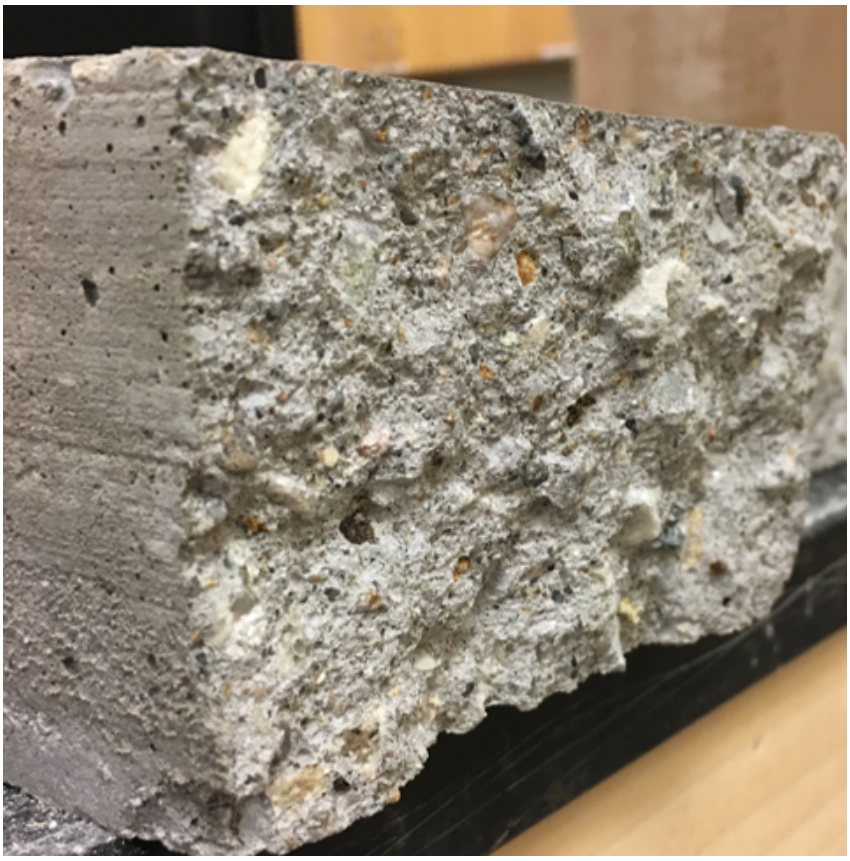

Figure 57 - Specimen #11 failure path

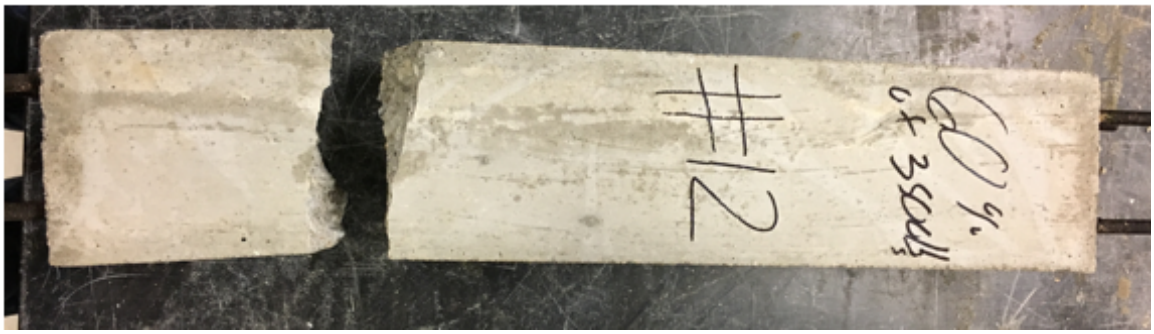

Figure 58 - Specimen #12 failure plan view

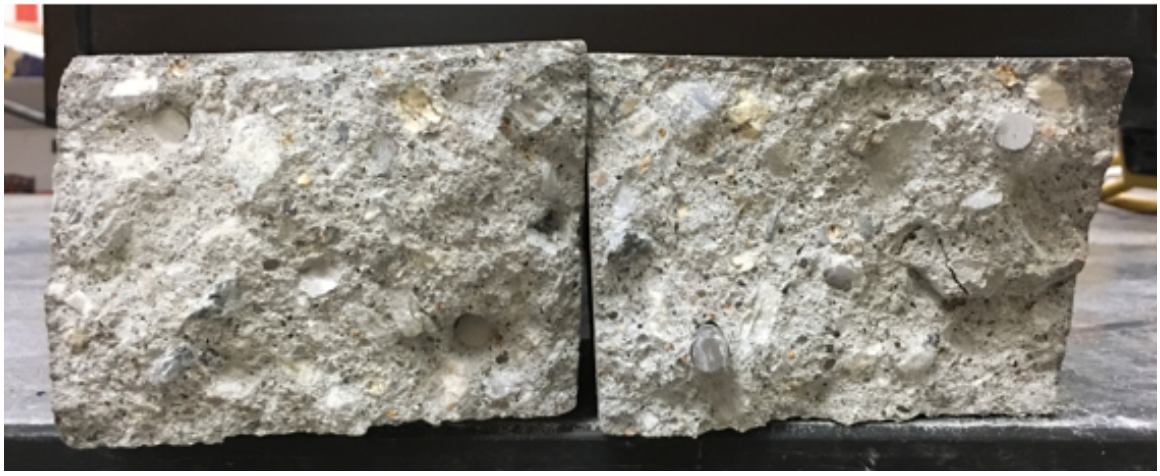

Figure 59 - Specimen #12 failure cross-section

Figure 60 - Specimen #12 failure path

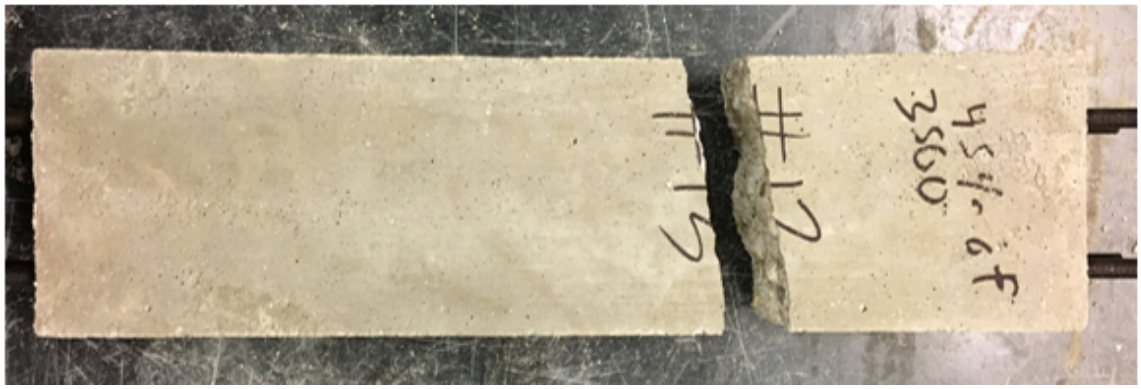

Figure 61 - Specimen #13 failure plan view

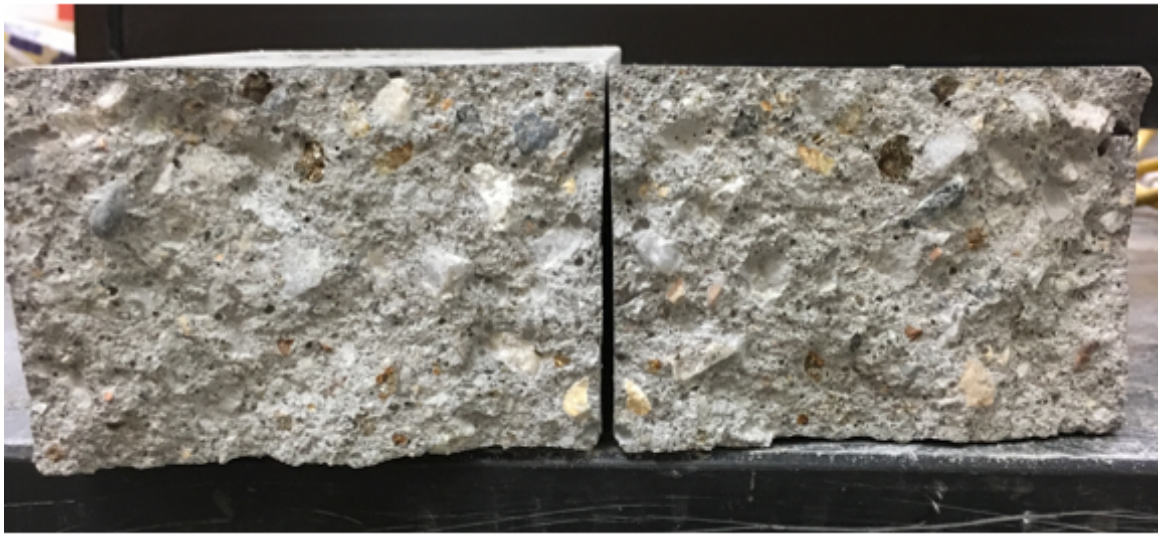

Figure 62 - Specimen #13 failure cross-section

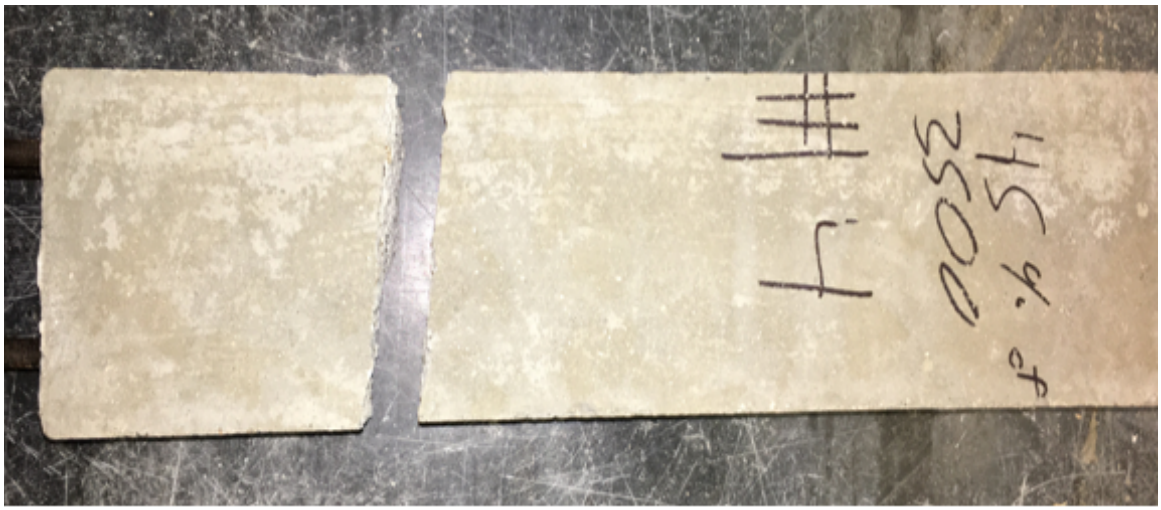

Figure 63 - Specimen #14 failure plan view

Figure 64 - Specimen #14 failure cross-section

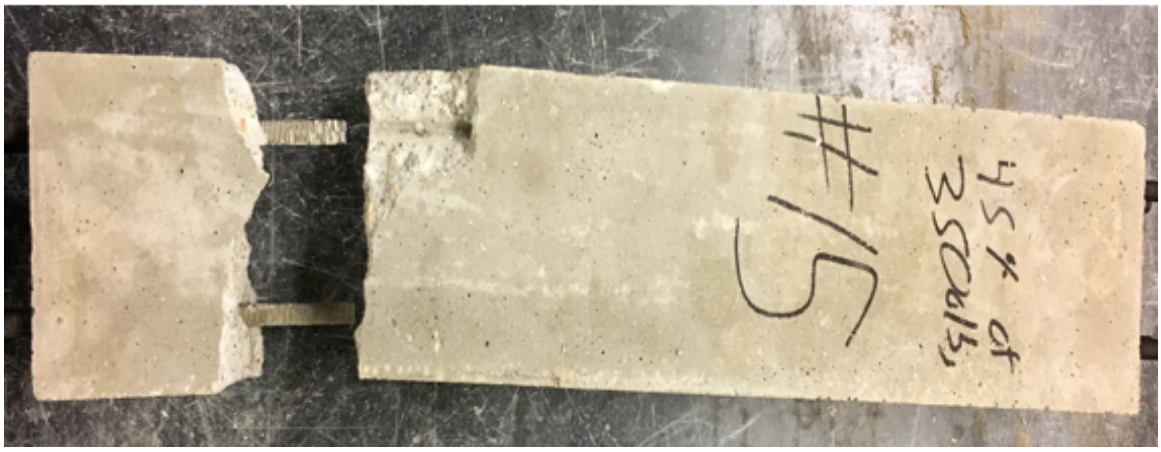

Figure 65 - Specimen #15 failure plan view

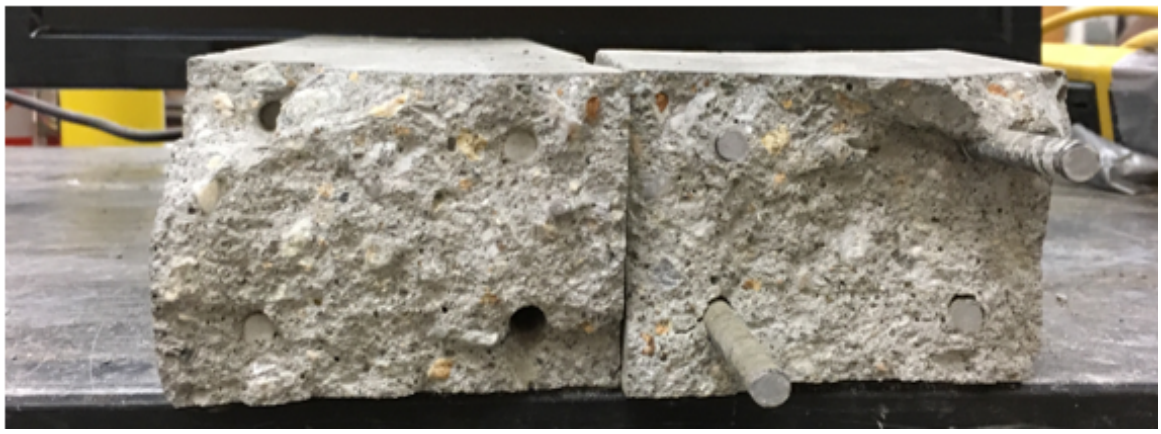

Figure 66 - Specimen #15 failure cross-section

Figure 67 - Specimen #16 failure plan view

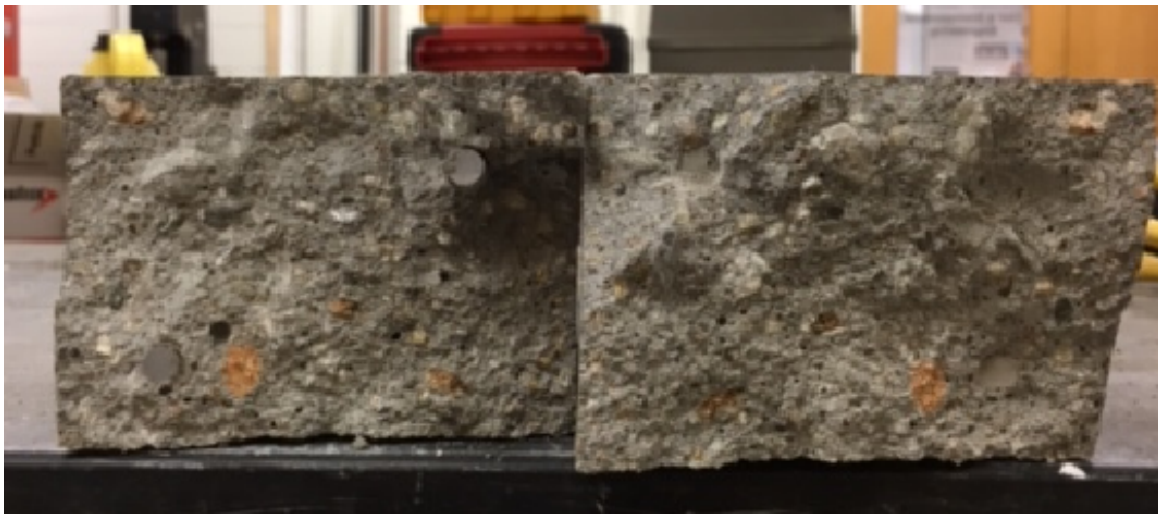

Figure 68 - Specimen #16 failure cross-section

Figure 69 - Specimen #17 failure plan view

Figure 70 - Specimen #17 failure cross-section

Figure 71 - Specimen #18 failure plan view

Figure 72 - Specimen #18 failure cross-section

Figure 73 - Specimen #19 failure plan view

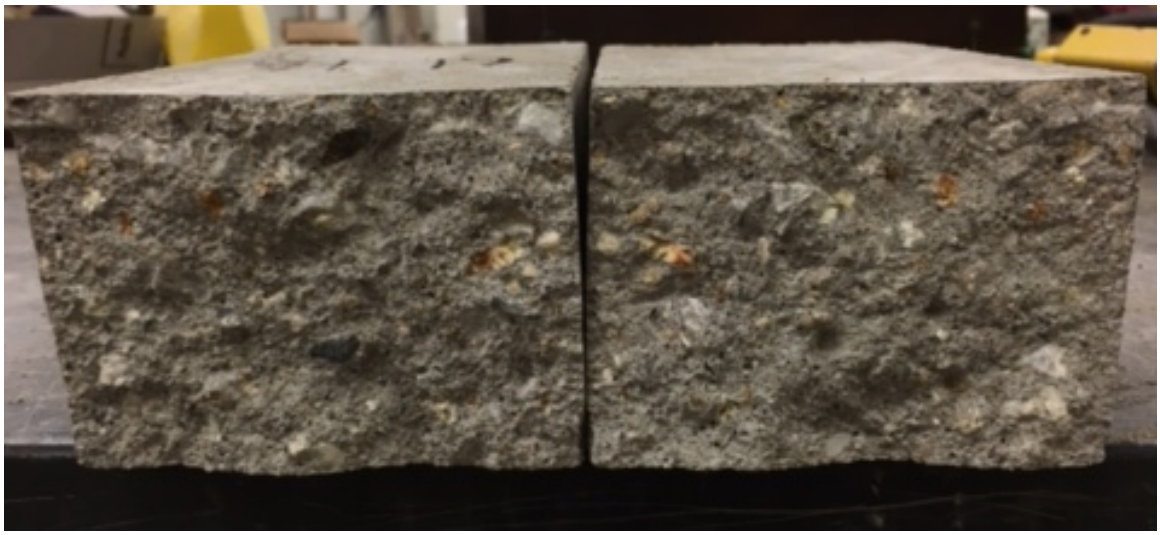

Figure 74 - Specimen #19 failure cross-section

Figure 75 - Specimen #20 failure plan view

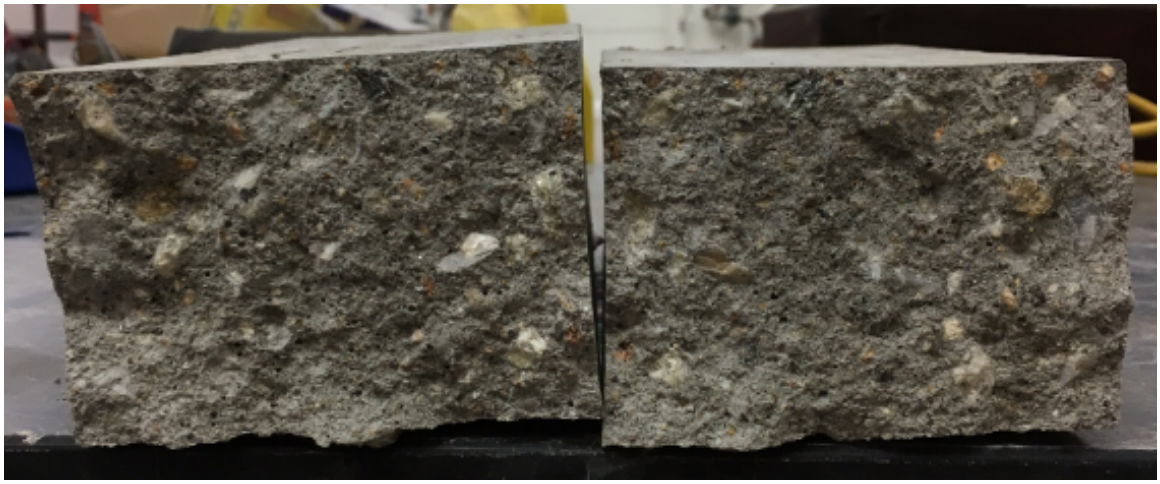

Figure 76 - Specimen #20 failure cross-section

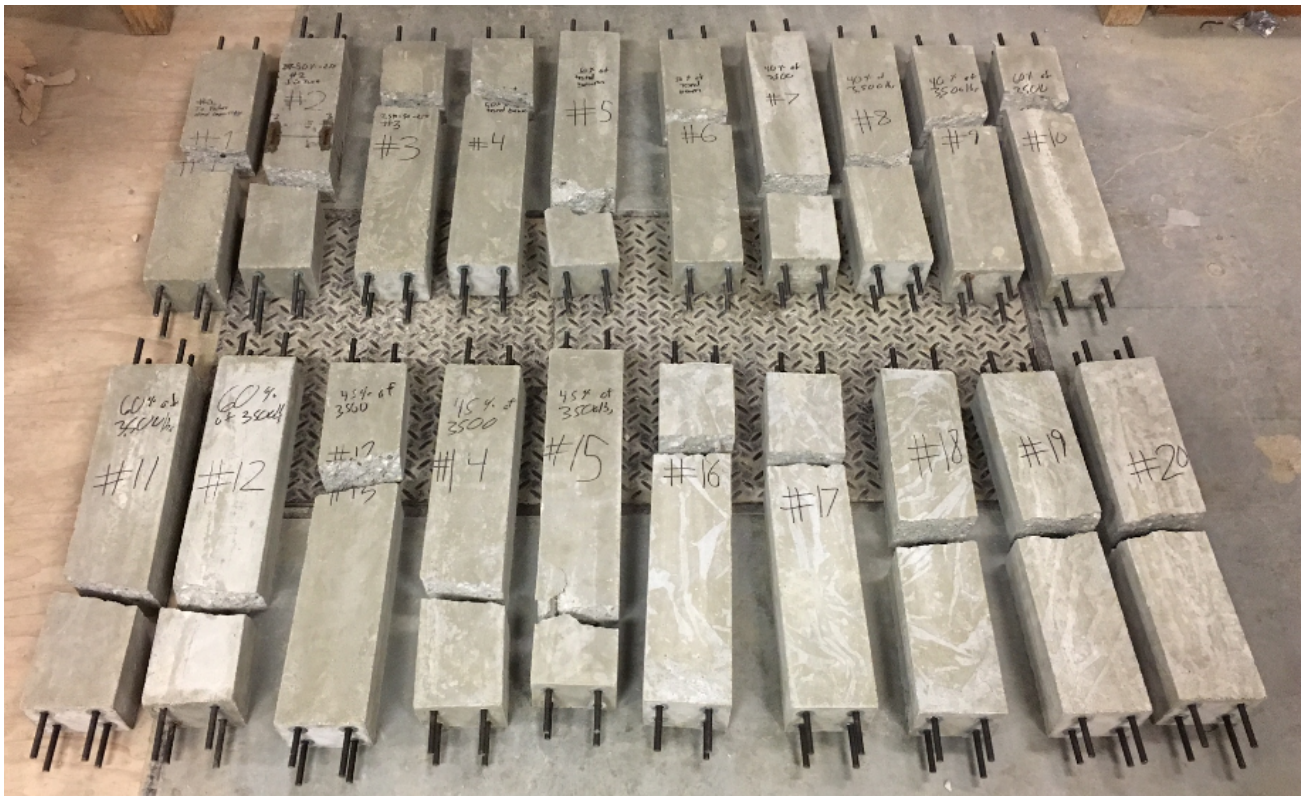

Figure 77 - All specimens tested

Appendix B

Table 5 - Thesis Dataset

Specimen Number	σmin / fr	σmax / fr	Number of Cycles Until Failure
1	To failure	To failure	NA
2	0.31	0.93	412
3	0.31	0.93	3439
4	0.31	0.93	199
5	0.31	0.93	0
6	0.31	0.93	6
7	0.24	0.73	22063
8	0.24	0.73	24369
9	0.24	0.73	2
10	0.55	0.93	2
11	0.55	0.93	84
12	0.55	0.93	75
13	0.26	0.81	27450
14	0.26	0.81	604
15	0.26	0.81	11
16	0.55	0.86	3620
17	0.55	0.86	34
18	0.55	0.86	52426
19	0.26	0.86	9180
20	0.26	0.86	15102

Table 6 – [Cornelissen 1982] Dataset

Specimen Number	σmin / fr	σmax / fr	Number of Cycles Until Failure
1	0.2	0.7	74131
2	0.2	0.7	2570396
3	0.2	0.7	2454709
4	0.2	0.7	1000000
5	0.2	0.7	74131
6	0.2	0.7	2570396
7	0.2	0.7	851138
8	0.2	0.7	85114
9	0.2	0.75	4266

10	0.2	0.75	98
11	0.2	0.75	7943
12	0.2	0.75	5495
13	0.2	0.75	479
14	0.2	0.8	2570
15	0.2	0.8	3090
16	0.2	0.8	30200
17	0.2	0.8	324
18	0.2	0.8	209
19	0.2	0.8	87
20	0.2	0.8	81
21	0.2	0.85	398
22	0.2	0.85	10
23	0.2	0.85	174
24	0.2	0.9	132
25	0.2	0.9	955
26	0.2	0.9	28
27	0.2	0.9	20
28	0.3	0.7	2630268
29	0.3	0.7	1995262
30	0.3	0.7	2089296
31	0.3	0.7	1513561
32	0.3	0.7	2291
33	0.3	0.75	14125
34	0.3	0.75	2089296
35	0.3	0.75	2570396
36	0.3	0.75	5495409
37	0.3	0.75	11482
38	0.3	0.75	3020
39	0.3	0.75	603
40	0.3	0.75	4677
41	0.3	0.8	2291
42	0.3	0.8	512861
43	0.3	0.8	1905461
44	0.3	0.8	489779
45	0.3	0.8	407380
46	0.3	0.8	831764
47	0.3	0.8	8511
48	0.3	0.8	10000
49	0.3	0.8	851
50	0.3	0.8	81

51	0.3	0.8	427
52	0.3	0.85	661
53	0.3	0.85	3020
54	0.3	0.85	170
55	0.3	0.85	166
56	0.3	0.85	407
57	0.3	0.9	44
58	0.3	0.9	288
59	0.3	0.9	1549
60	0.3	0.9	12
61	0.3	0.9	25
62	0.3	0.9	28
63	0.3	0.9	68
64	0.3	0.9	550
65	0.4	0.7	2041738
66	0.4	0.7	3090295
67	0.4	0.7	2089296
68	0.4	0.7	2511886
69	0.4	0.75	5495
70	0.4	0.8	1288
71	0.4	0.8	213796
72	0.4	0.8	1995262
73	0.4	0.8	2884032
74	0.4	0.8	60256
75	0.4	0.8	4169
76	0.4	0.8	3311
77	0.4	0.8	1549
78	0.4	0.8	1698
79	0.4	0.85	912
80	0.4	0.9	7079
81	0.4	0.9	169824
82	0.4	0.9	501
83	0.4	0.9	708
84	0.4	0.9	30
85	0.4	0.9	832
86	0.4	0.9	135
87	0.4	0.9	1122